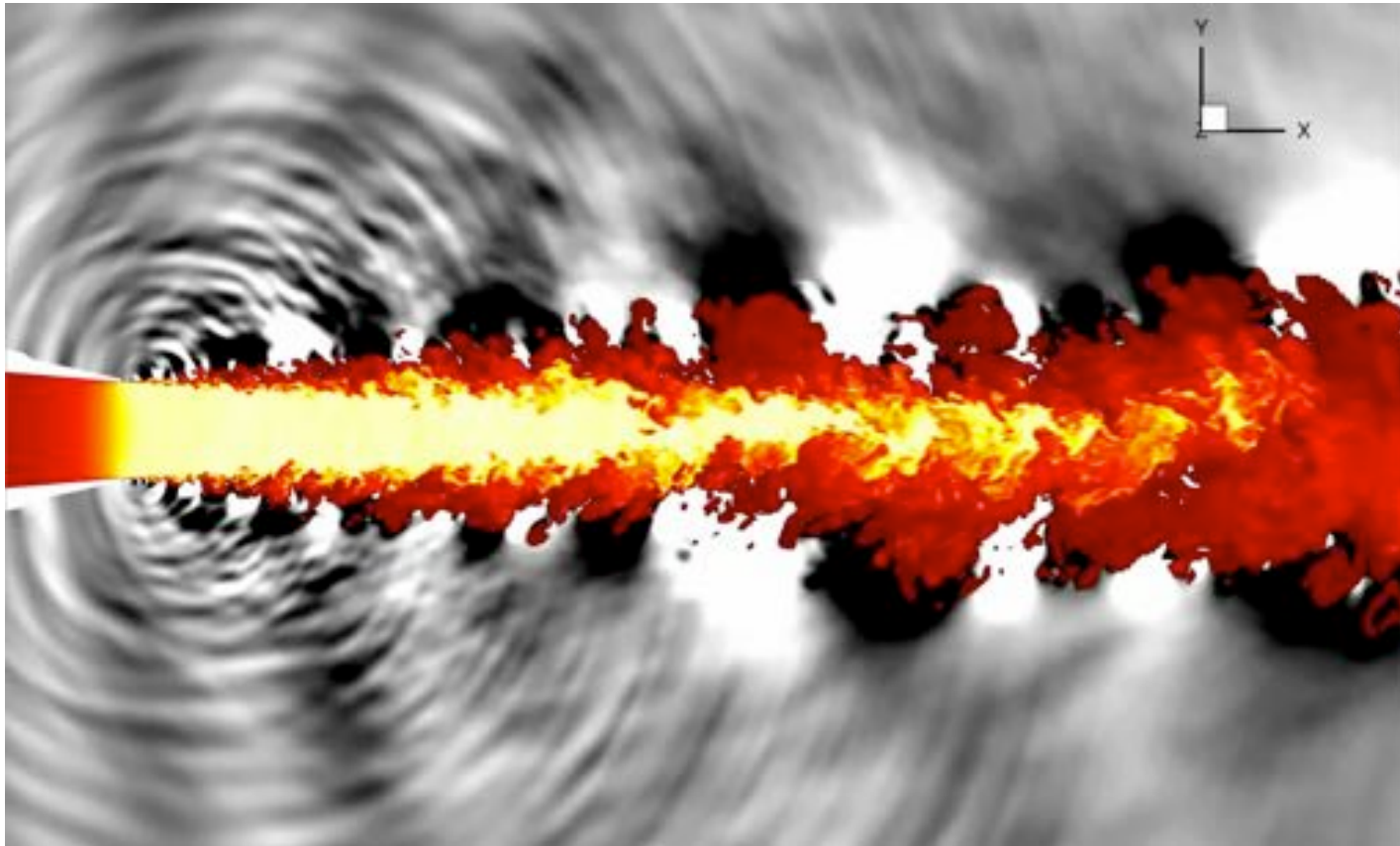


Jet Noise Prediction using Hybrid RANS/LES with Structured Overset Grids



Jeffrey Housman¹, Gerrit-Daniel Stich², Cetin Kiris¹, and James Bridges³

1. Computational Aerosciences Branch, NASA Ames Research Center
2. Science and Technology Corporation, NASA Ames Research Center
3. Aeroscience Branch, NASA Glenn Research Center

AIAA Aviation 2017, Denver, Colorado
Session: AA-15, Jet Noise II: CFD Supersonic
June 5, 2017

Outline



- Introduction
- Experimental Setup
- Computational Methodology
- Structured Overset Grid System
- Computational Results
 - Near-Field Comparison
 - Far-Field Comparison
- Summary
- Future Work

Introduction

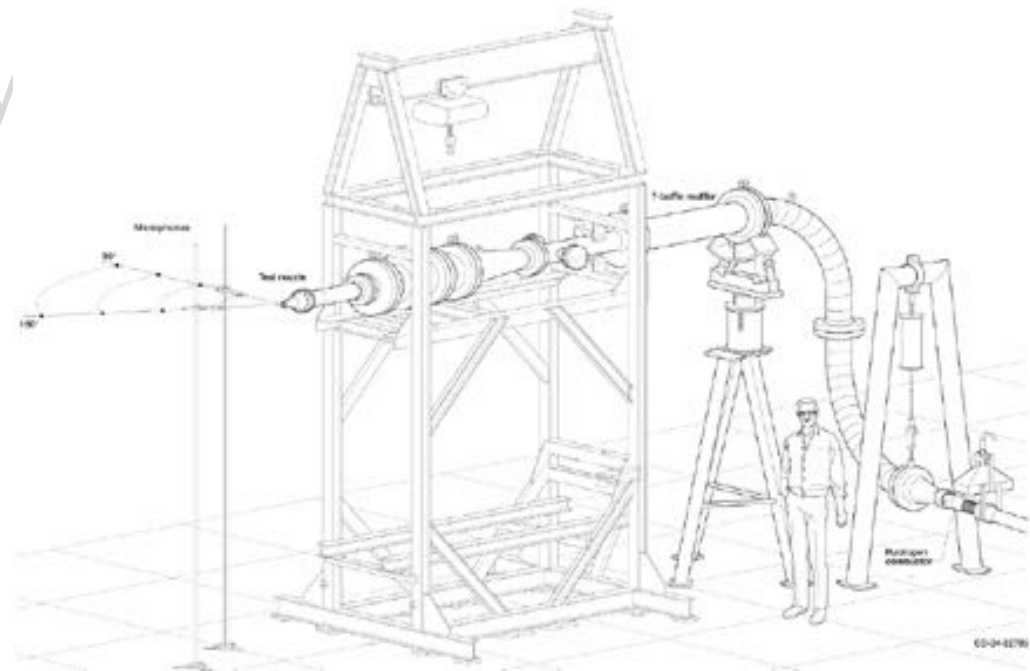


- NASA has initiated the development of quiet supersonic business Jets
- Return of commercial supersonic flight will allow passengers to travel over the continental U.S. within hours and complete international business trips within a single day.
- NASA awarded contract for preliminary design of a low boom flight demonstrator for Quiet Supersonic Technology project (QueSST)
- Most efforts of the design are focused on reducing the sonic boom ground signature, however the noise constraints during takeoff and landing at subsonic speeds must be satisfied.
- Computational aeroacoustic (CAA) tools can be used to assess the new designs at lower speeds.
- This work represents the first part of a systematic validation effort in jet noise prediction capability for NASA Ames Launch Ascend and Vehicle Aerodynamics Code (LAVA).

Outline



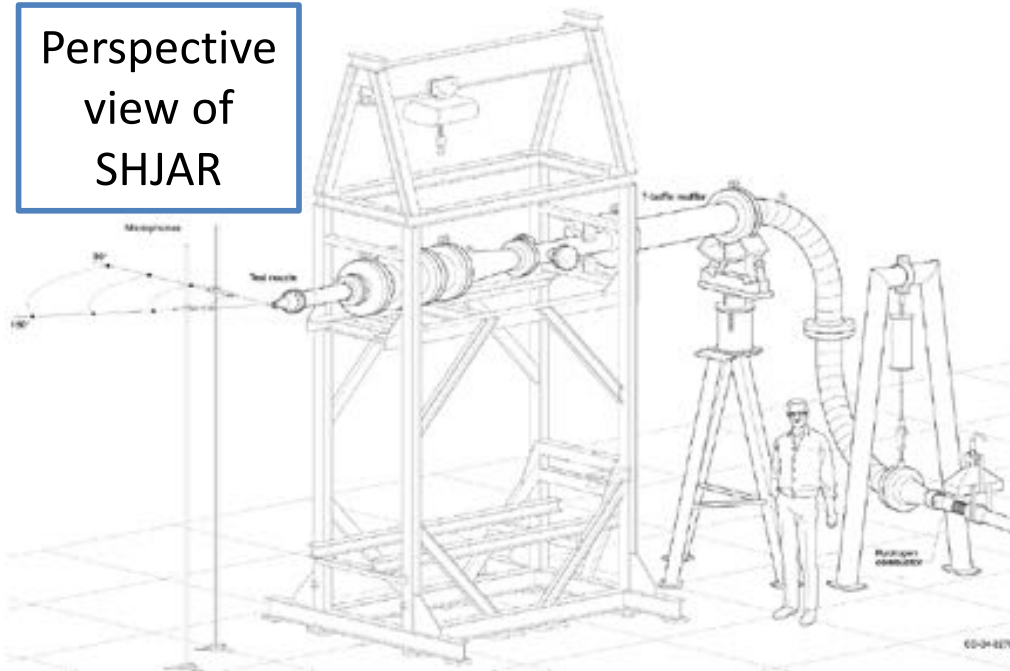
- Introduction
- **Experimental Setup**
- Computational Methodology
- Structured Overset Grid System
- Computational Results
 - Near-Field Comparison
 - Far-Field Comparison
- Summary
- Future Work



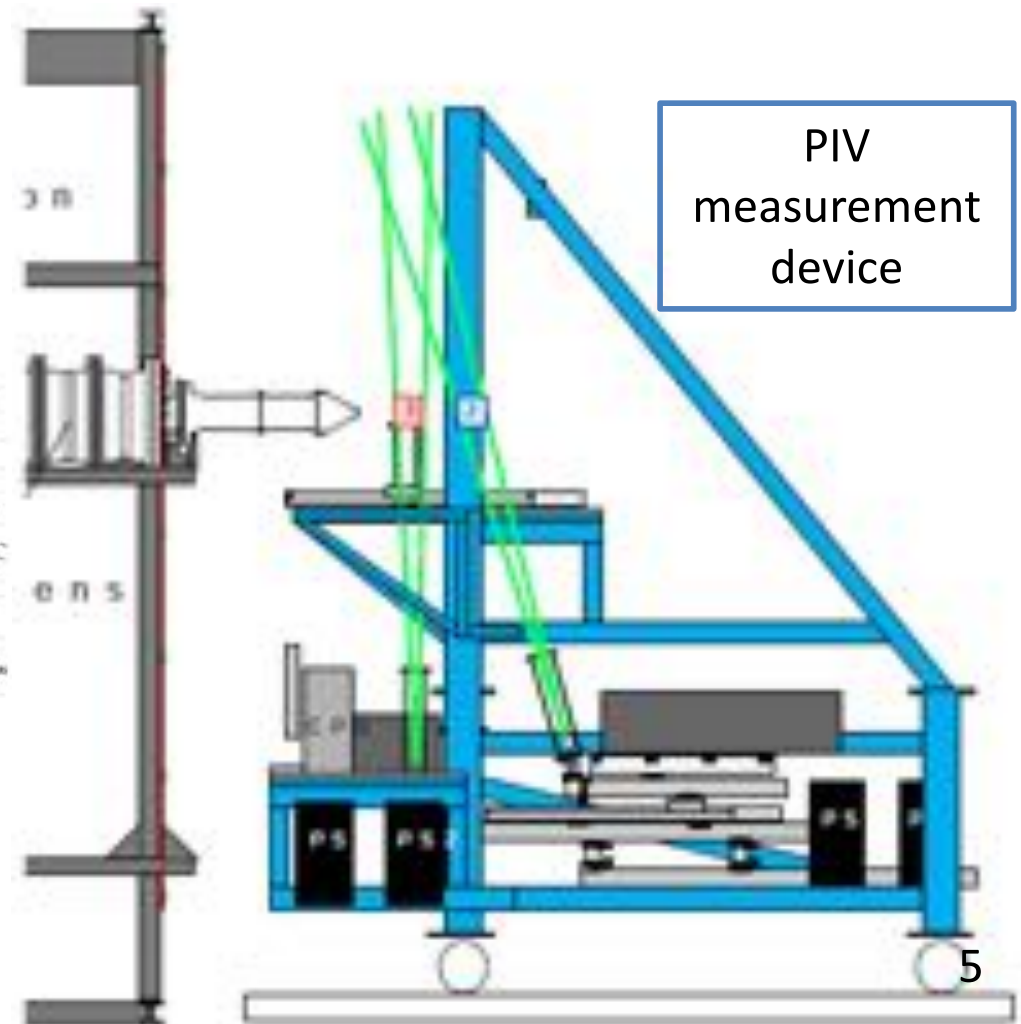
Experimental Setup

- Small Hot Jet Acoustic Rig (SHJAR), which is located in the Aeroacoustics Propulsion Lab (AAPL) at NASA Glenn Research Center

Perspective
view of
SHJAR



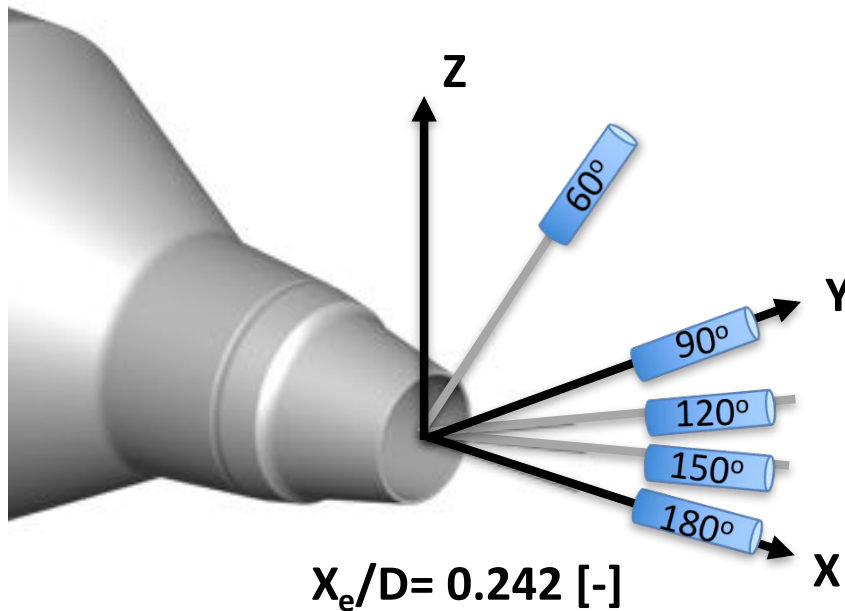
PIV
measurement
device



Bridges et. al. (NASA-TM-2011-216807)

Experimental Setup

- Baseline axisymmetric convergent Small Metal Chevron (SMC000) nozzle at Set Point 7 (SP7)
- Nozzle axis in downstream flow direction is marked as 180°

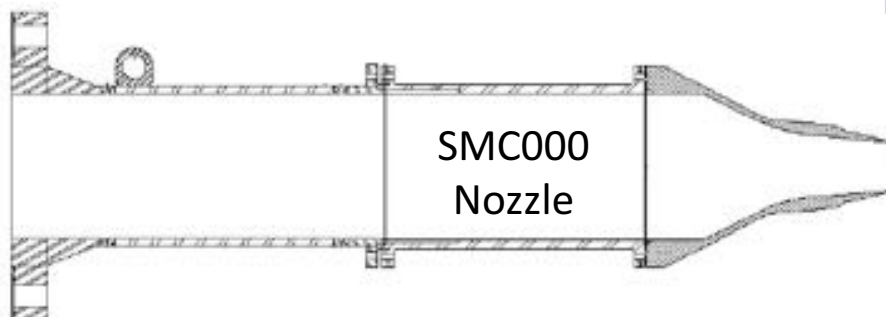


Bridges et. al. (NASA-TM-2011-216807)	SP7
Acoustic Mach number U_{jet}/c	0.9
Jet temperature ratio T_e/T	0.835
Nozzle pressure ratio NPR	1.861
Nozzle Diameter D	0.0508 [m] 2.0 [inch]
Reynold number Re_D	1 Mio
Reynolds number Re	800
Boundary layer thickness	0.0128 D

similar to: Bres et. al. (AIAA-2015-2535)

“Bruit et vent” jet-noise facility at

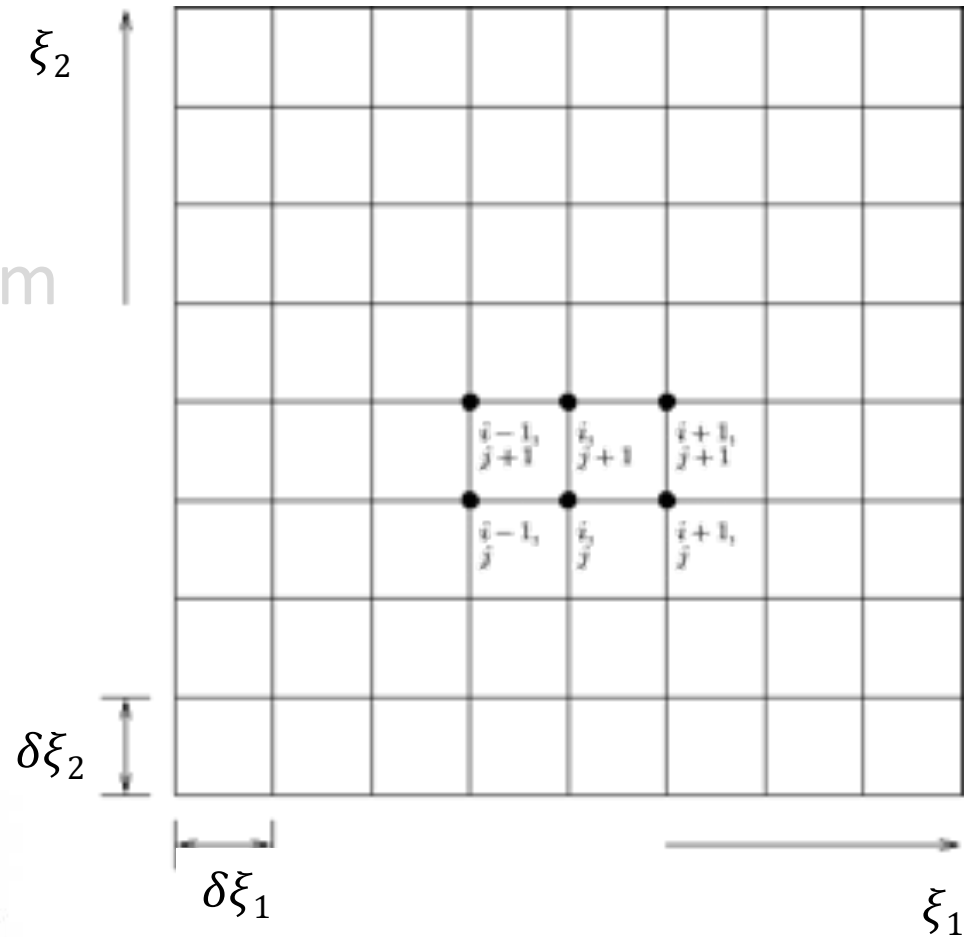
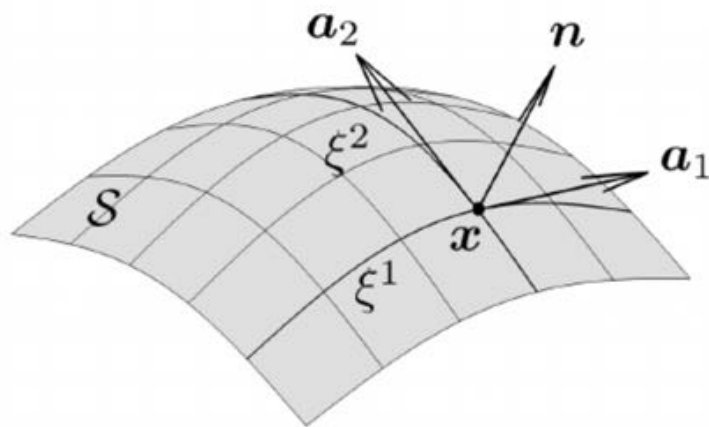
Centre d’Etudes Aerodynamique et Termique



Outline



- Introduction
- Experimental Setup
- **Computational Methodology**
- Structured Overset Grid System
- Computational Results
 - Near-Field Comparison
 - Far-Field Comparison
- Summary
- Future Work

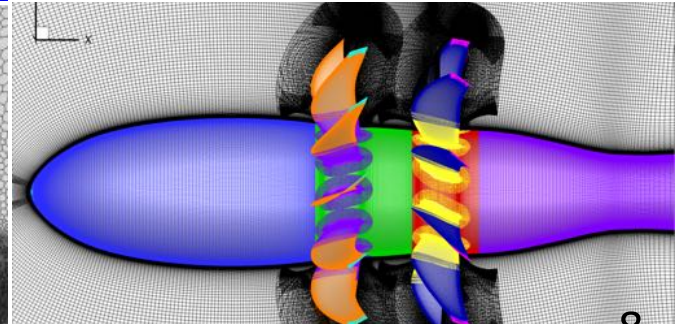
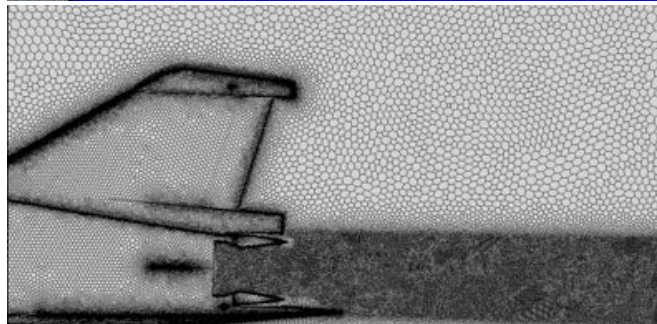
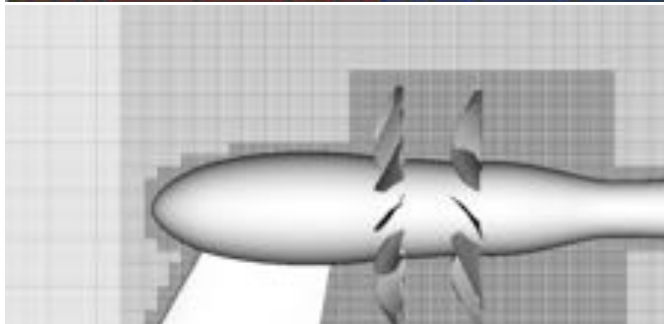
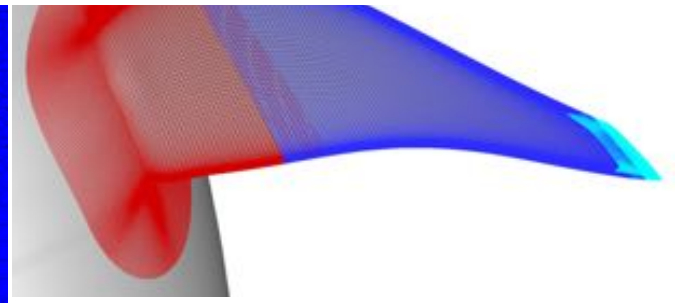
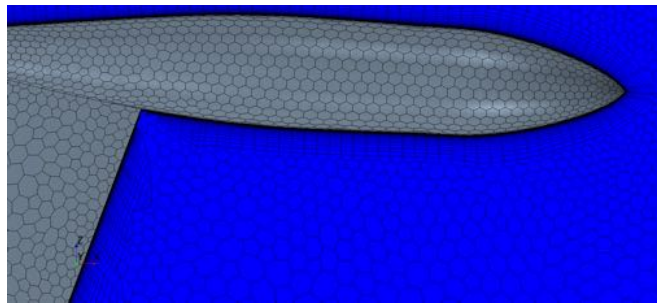
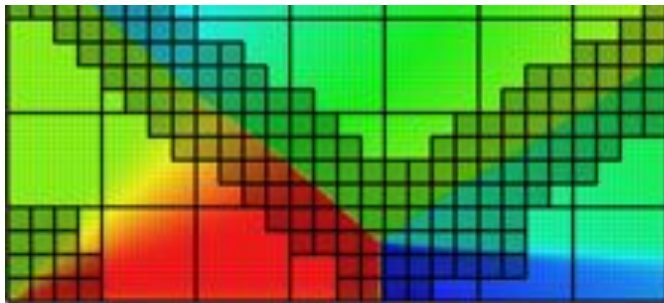


Computational Methodology



LAVA Framework (Kiris et al. Aerospace Science and Technology, Volume 55, 2016)

- Computational Fluid Dynamics Solvers
 - Cartesian, Curvilinear, and Unstructured Grid Types
 - Overset Grid and Immersed Boundary Methods
 - Steady and Unsteady RANS (Reynolds Averaged Navier-Stokes)
 - Hybrid RANS/LES (Large Eddy Simulation), LES and LBM Capabilities
- Acoustic Solver
 - Linear Helmholtz Scattering Code
 - Permeable Surface Flow Williams-Hawkins Propagation



Cartesian Immersed Boundary

Unstructured Arbitrary Polyhedral

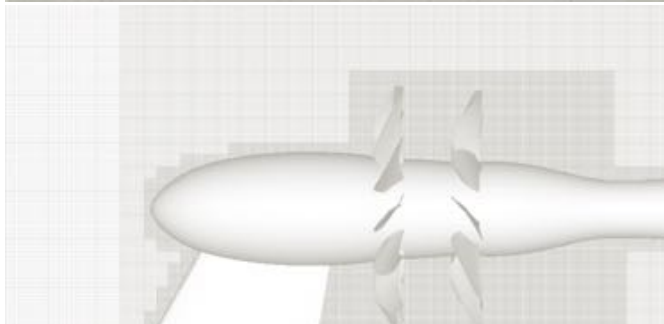
Overset Structured Curvilinear

Computational Methodology

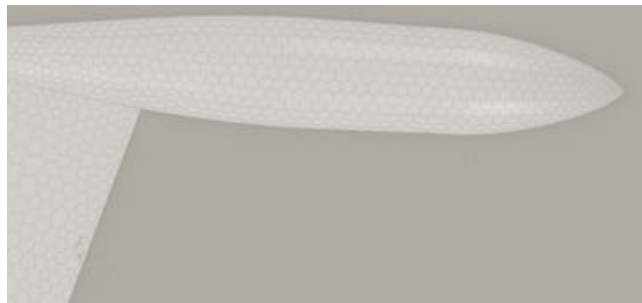


LAVA Framework (Kiris et al. Aerospace Science and Technology, Volume 55, 2016)

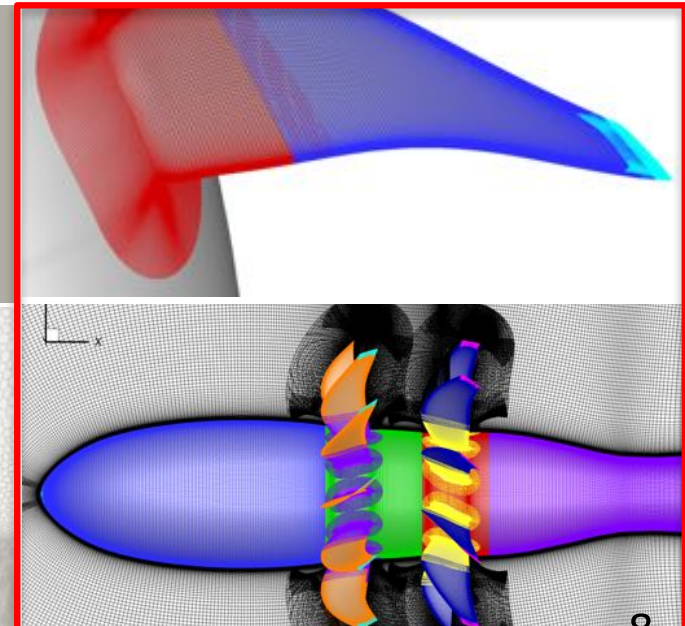
- Computational Fluid Dynamics Solvers
 - Cartesian, **Curvilinear**, and Unstructured Grid Types
 - **Overset Grid** and Immersed Boundary Methods
 - Steady and **Unsteady RANS** (Reynolds Averaged Navier-Stokes)
 - **Hybrid RANS/LES** (Large Eddy Simulation), LES and LBM Capabilities
- Acoustic Solver
 - Linear Helmholtz Scattering Code
 - **Permeable Surface Flow Williams-Hawkins Propagation**



Cartesian Immersed Boundary



Unstructured Arbitrary Polyhedral



Overset Structured Curvilinear

Computational Methodology



3-D Structured Curvilinear Overset Grid Solver

- Spalart-Allmaras turbulence model (baseline turbulence model)

Low-Dissipation Finite Difference Method (Housman et al. AIAA-2016-2963)

- 6th-order Hybrid Weighted Compact Nonlinear Scheme (HWCNS)
- Numerical flux is a modified Roe scheme
- 6th/5th-order blended central/upwind biased left and right state interpolation
- 2nd-order accurate differencing used for time discretization

Hybrid RANS/LES Models

- Delayed Detached Eddy Simulation (DDES) model with modified length scale (Housman et al. AIAA-2017-0640)
- Zonal RANS-NLES (numerical LES) with user selected zones of URANS, NLES, and wall-distance based hybrid RANS-NLES (see paper for details)

Synthetic Eddy Method

- *Coupling Methodology between RANS and LES to introduce realistic turbulent eddies* (Jarrin et al. Int. Journal of Heat and Fluid Flow 30)

Computational Methodology

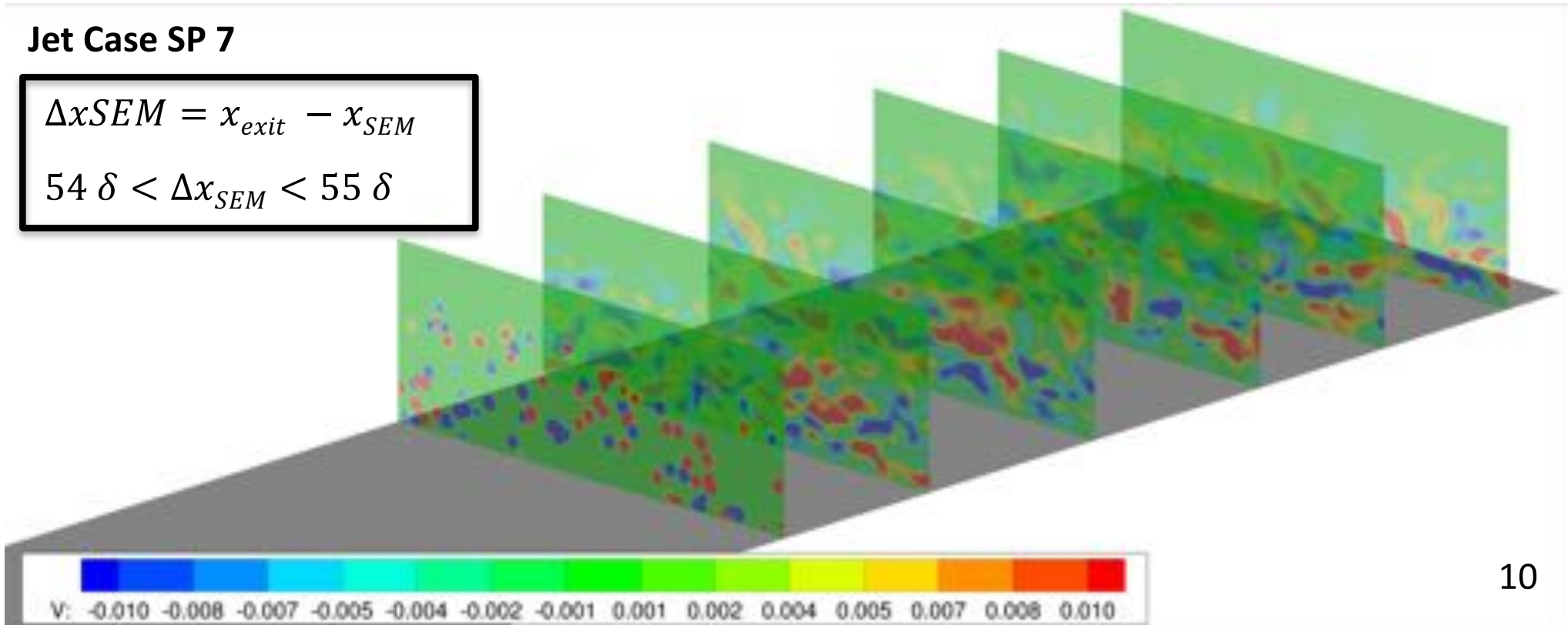


- When transitioning from RANS to LES in wall-bounded flows it is necessary to insert meaningful three-dimensional content at the interface
- The synthetic eddy method (SEM) is one approach which adds eddies in such away that first and second order turbulent statistics can be satisfied. (approx. from the RANS solution with Bradshaw hypothesis)

Jet Case SP 7

$$\Delta x_{SEM} = x_{exit} - x_{SEM}$$

$$54 \delta < \Delta x_{SEM} < 55 \delta$$



Computational Methodology



uRANS

$\Delta t = 1 \cdot 10^{-4}$ [s] ; 0.4 [s]



initialize Hybrid
RANS/LES

$\Delta t = 1 \cdot 10^{-6}$ [s] ; nt > 30000



final Hybrid
RANS/LES

$\Delta t = 1 \cdot 10^{-6}$ [s]

$St_{\max} = 16.25$, $St_{\min} = 0.008$

$T_{conv} \approx 205$

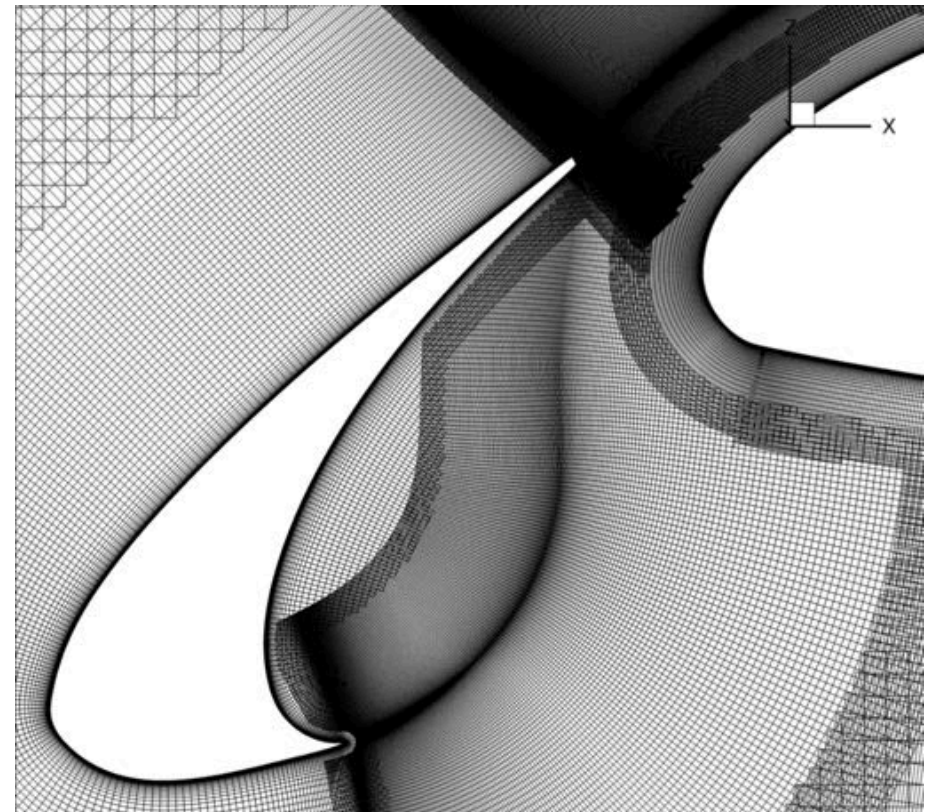
- Unsteady RANS until jet is fully developed and eddy viscosity maximum has plateaued
- Restart simulation with Hybrid RANS/LES Models until transient behavior washed out
- Ignore transients which are taken at first 30000 time-steps and restart simulation
- Record Volume data at 100 kHz sampling frequency for greater than 0.02 seconds (approx. 205 convective time units)

	baseline	coarse	refined
Processors	1392 (has)	260 (ivy)	960 (has)
Wall-Clock Time [day]	12.5		
Sub-iterations	5		
Convergence	2-4 orders every sub-iteration		
Number Eddies (SEM)	-	5000	5000

Outline



- Introduction
- Experimental Setup
- Computational Methodology
- **Structured Overset Grid System**
- Computational Results
 - Near-Field Comparison
 - Far-Field Comparison
- Summary
- Future Work



Structured Overset Grid System

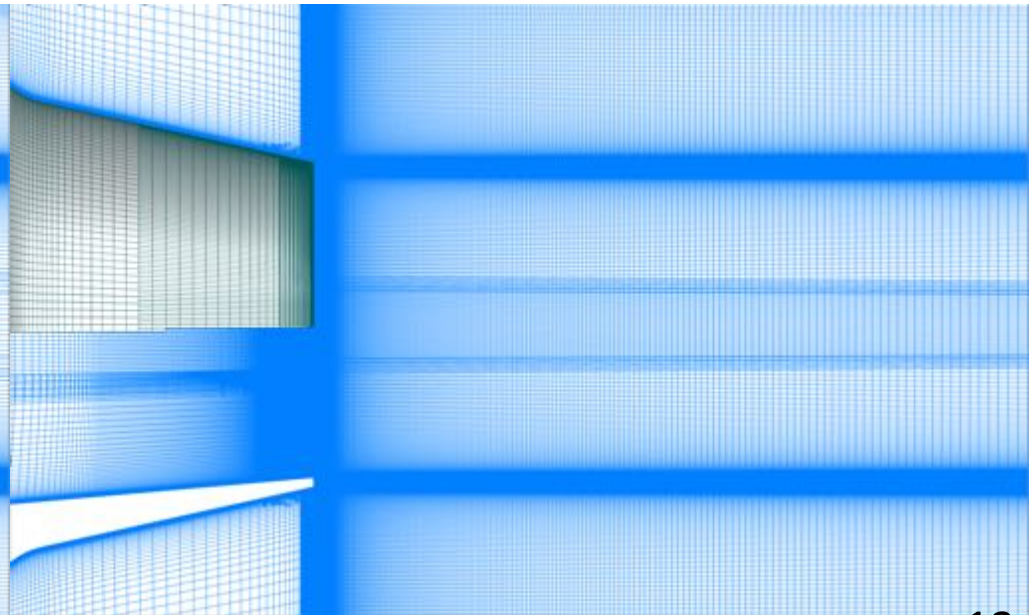


Baseline (256 M)

- Baseline (256 M)
- Coarse (28 M)
- Refined (106 M)
- Seven point overlap
- No orphan points
- Minimum stencil quality 0.9
- Baseline follows Bogey et. al (AIAA-2016-0261)



Coarse (28 M)



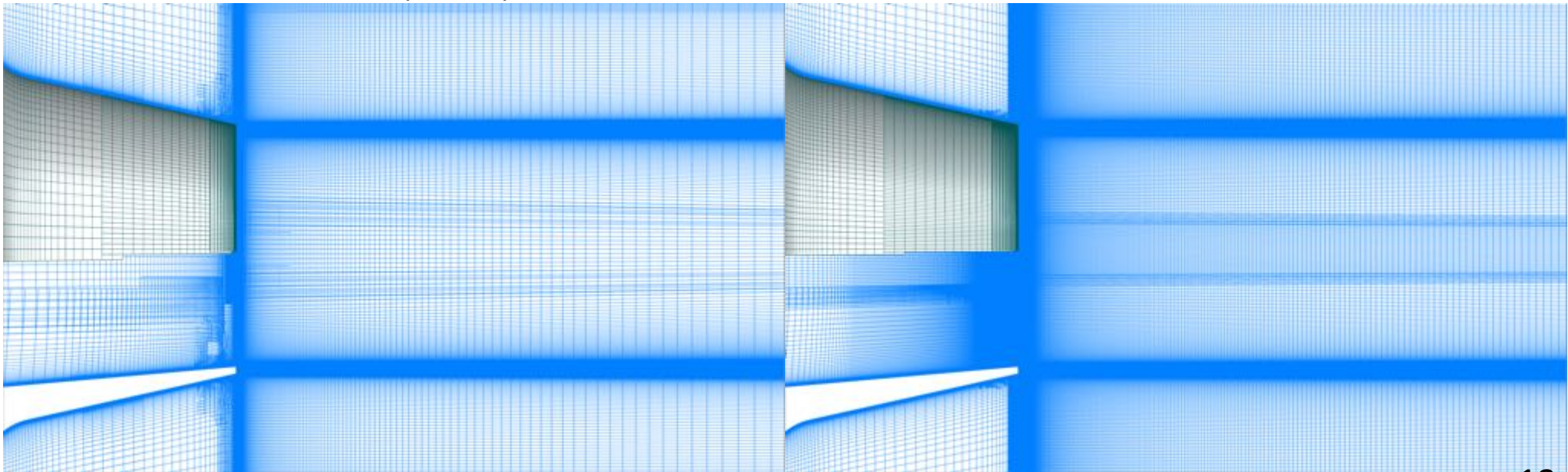
Refined (106 M)

Structured Overset Grid System



Baseline (256 M)

- Circumferential refinement in axial and radial direction
Bres *et. al.* (AIAA-2015-2535)



Coarse (28 M)

Refined (106 M)

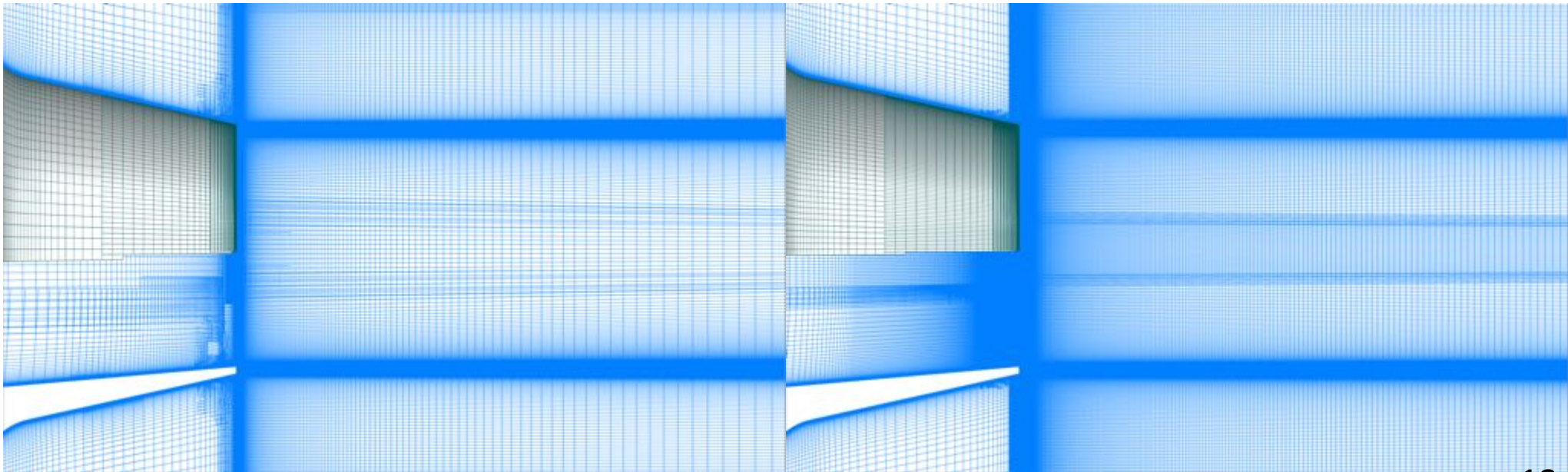
Structured Overset Grid System



circumferential
refinement



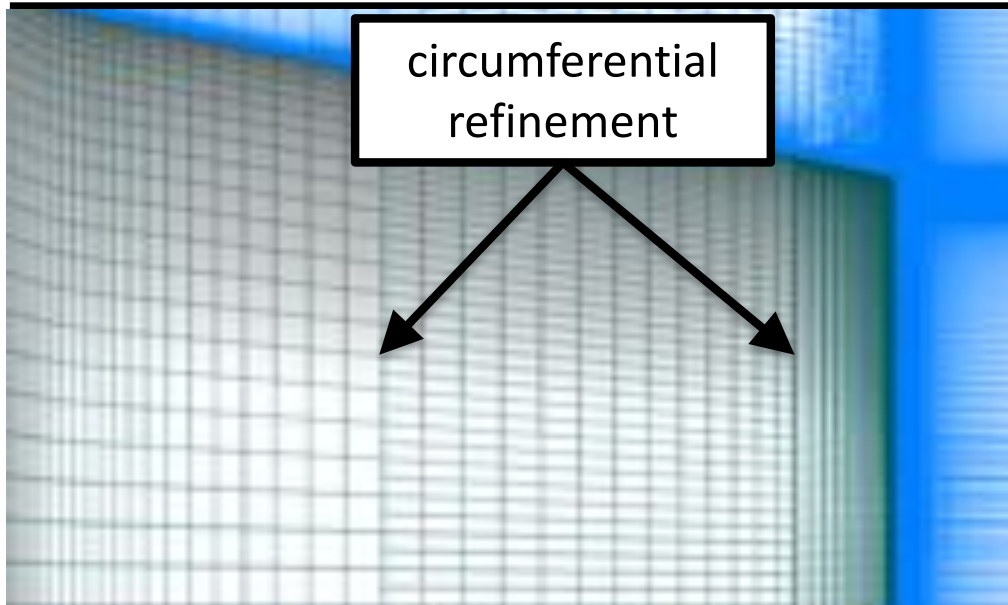
- Circumferential refinement in axial and radial direction
Bres *et. al.* (AIAA-2015-2535)



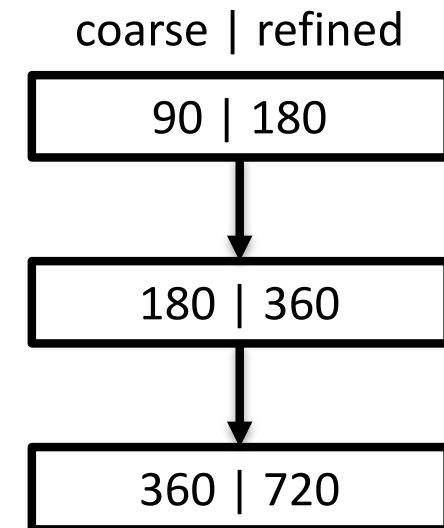
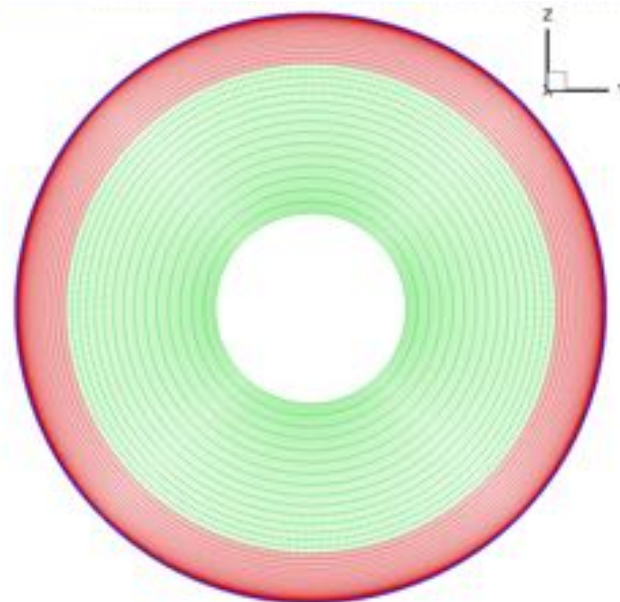
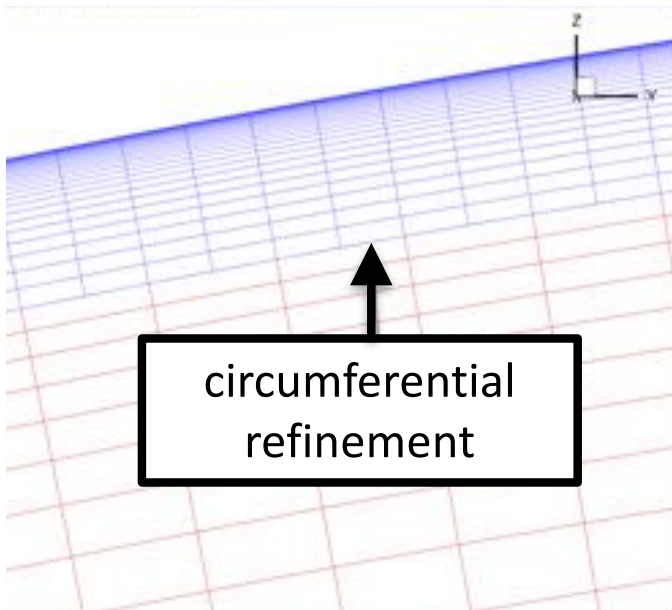
Coarse (28 M)

Refined (106 M)

Structured Overset Grid System

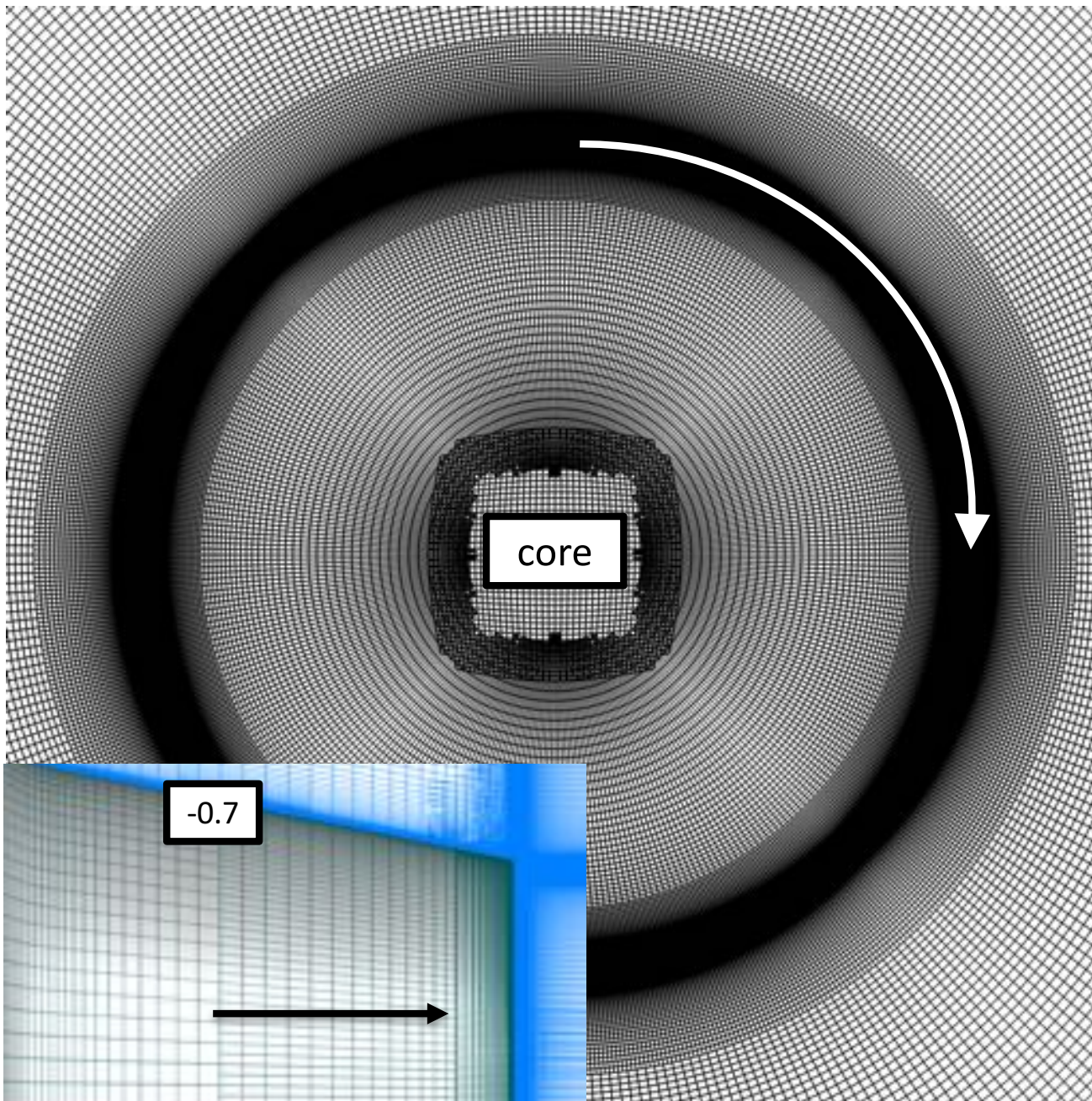


- Circumferential refinement in axial and radial direction
Bres *et. al.* (AIAA-2015-2535)



baseline 360

Structured Overset Grid System



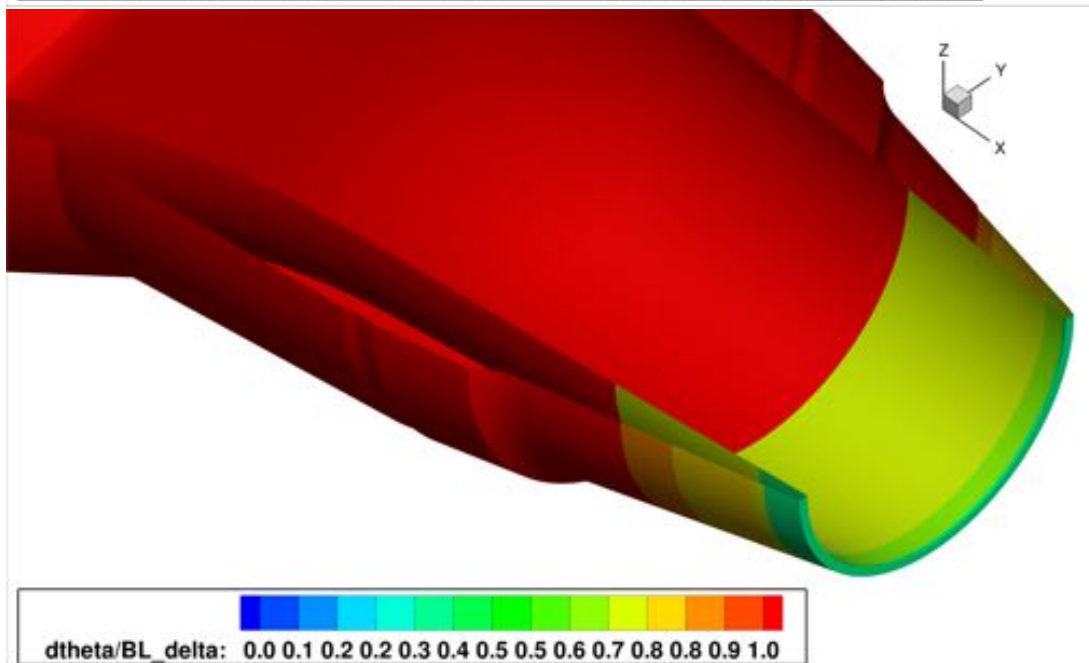
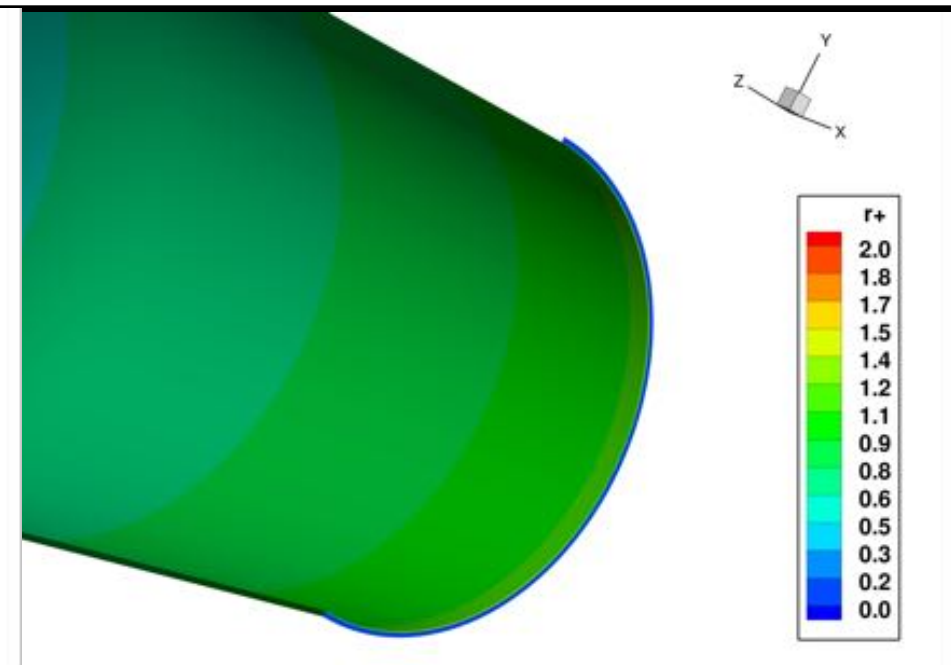
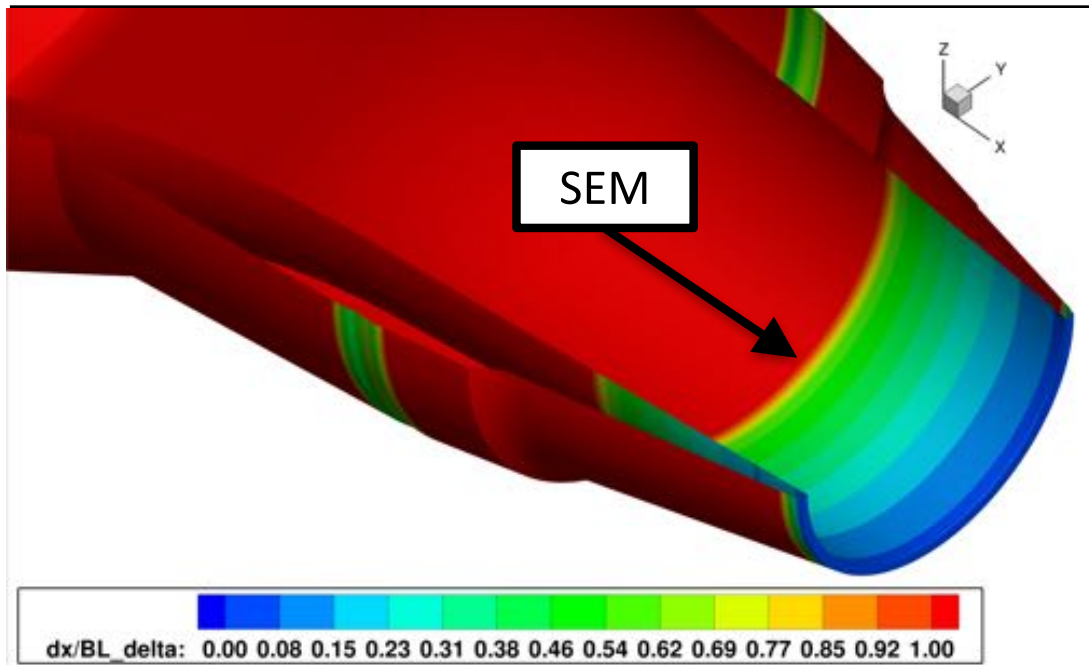
axial/radial AR

	$(x-x_{\text{exit}})/D$	AR
wall	-0.7	321.15
core	-0.7	0.50
wall	0.0	34.50
core	0.0	0.06
shear	0.5 – 25.0	10.50
core	0.5 – 25.0	1.05

circumferential/radial AR

	$(x-x_{\text{exit}})/D$	AR
wall	-0.7	436.82
core	-0.7	1.00
wall	0.0	221.00
core	0.0	1.00
shear	0.5 – 25.0	1134
core	0.5 – 25.0	1.00

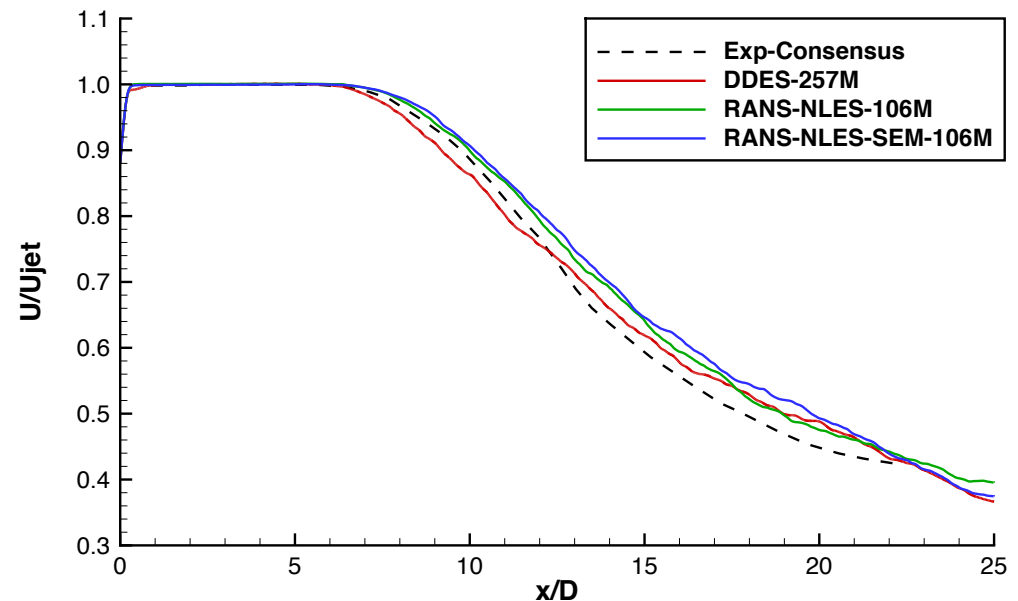
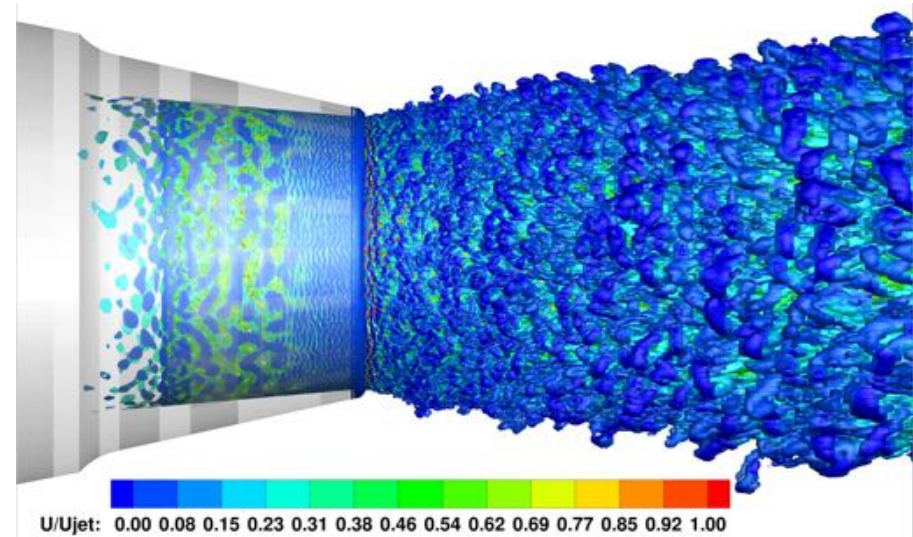
Structured Overset Grid System



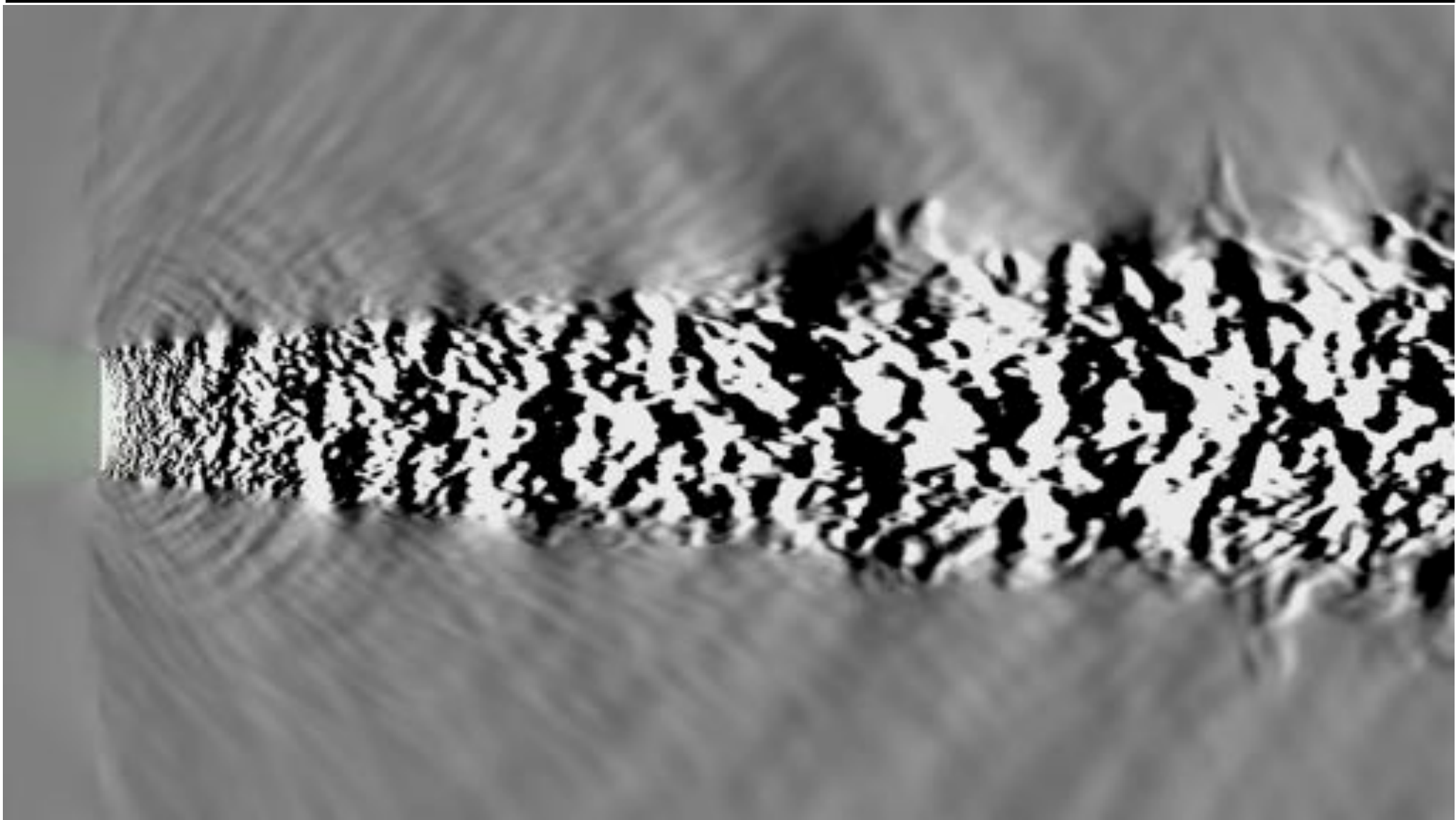
Outline



- Introduction
- Experimental Setup
- Computational Methodology
- Structured Overset Grid System
- **Computational Results**
 - Near-Field Comparison
 - Far-Field Comparison
- Summary
- Future Work



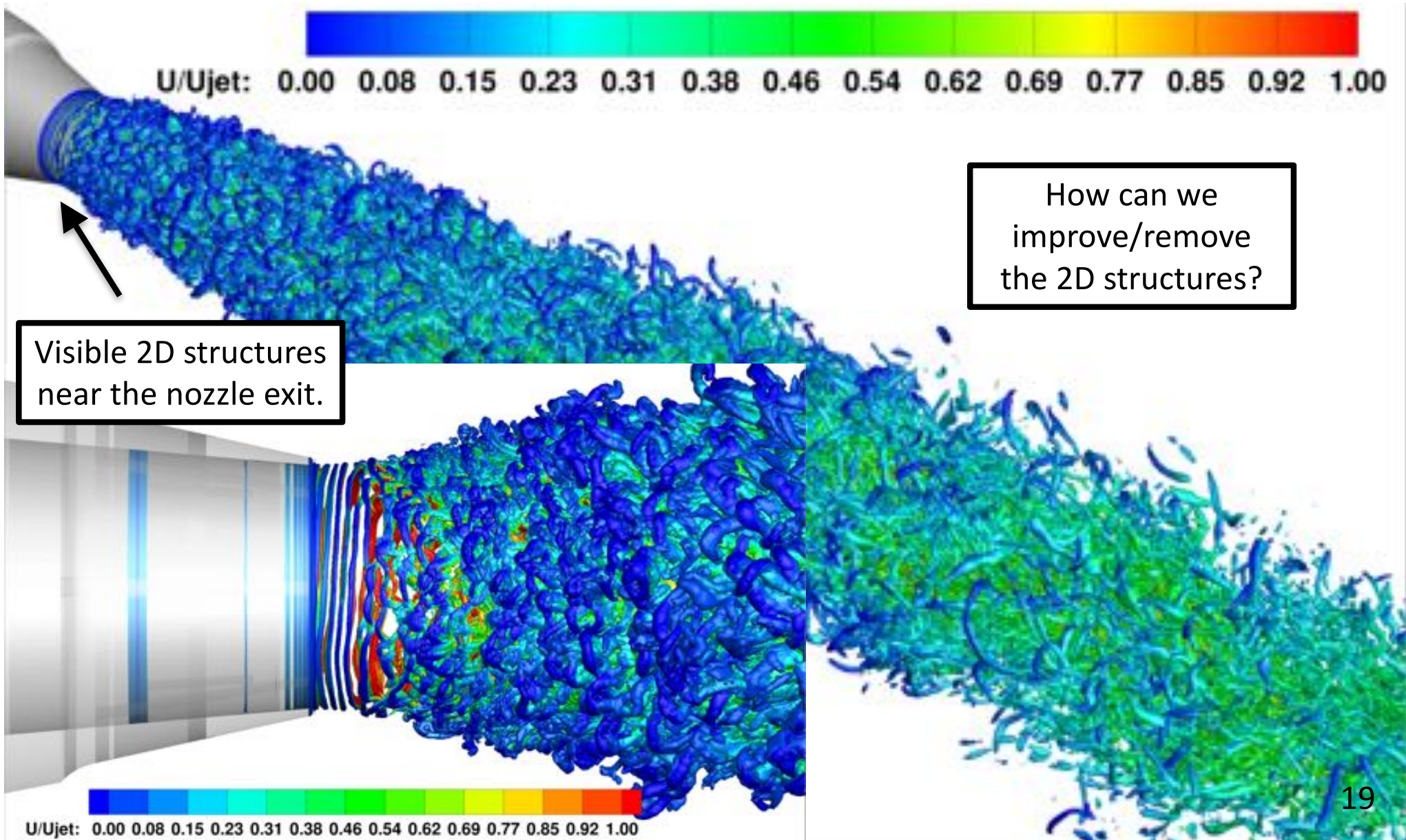
Computational Results



Computational Results

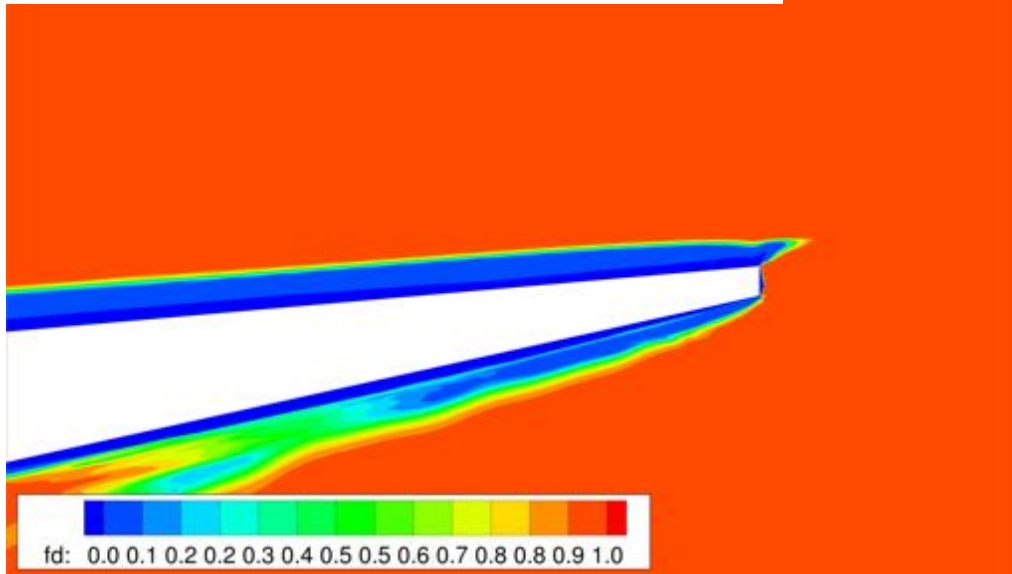


Flow Field Visualization: Iso-contour of Q-criteria colored by axial velocity

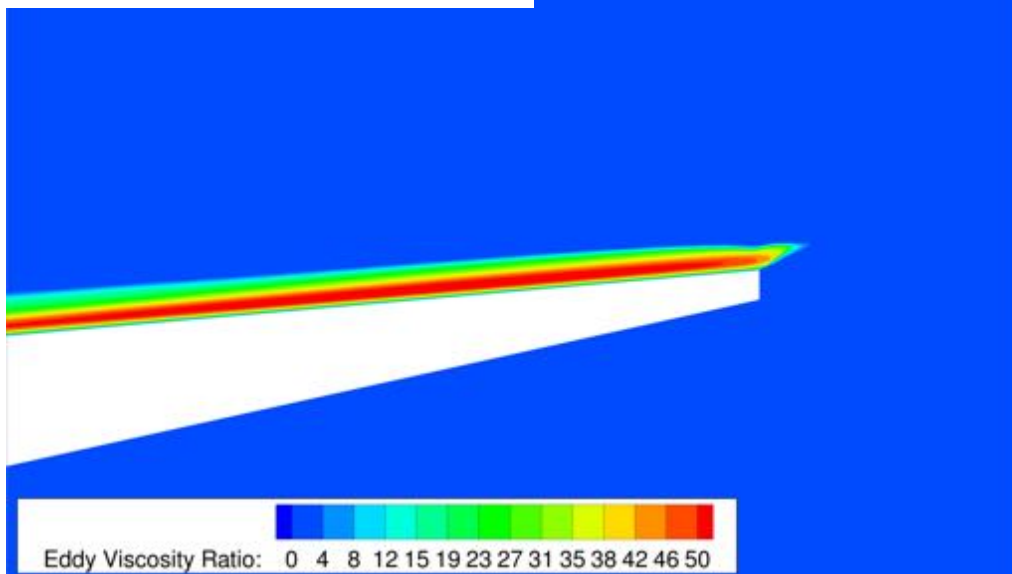


Computational Results

Indicator Function: DDES-256M



μ_T/μ_∞ : DDES-256M



- Indicator function f_d indicates if in RANS or LES mode.
- Stays in RANS mode in nozzle interior and quickly transitions to LES downstream of nozzle lip
- Retains large eddy viscosity throughout the boundary layer

- Shielding function RANS-NLES:

$$f_d = 1 - \frac{1}{2} \left[1 - \tanh(\epsilon_d(d_{wall} - d_0)) \right]$$

d_{wall} : walldistance

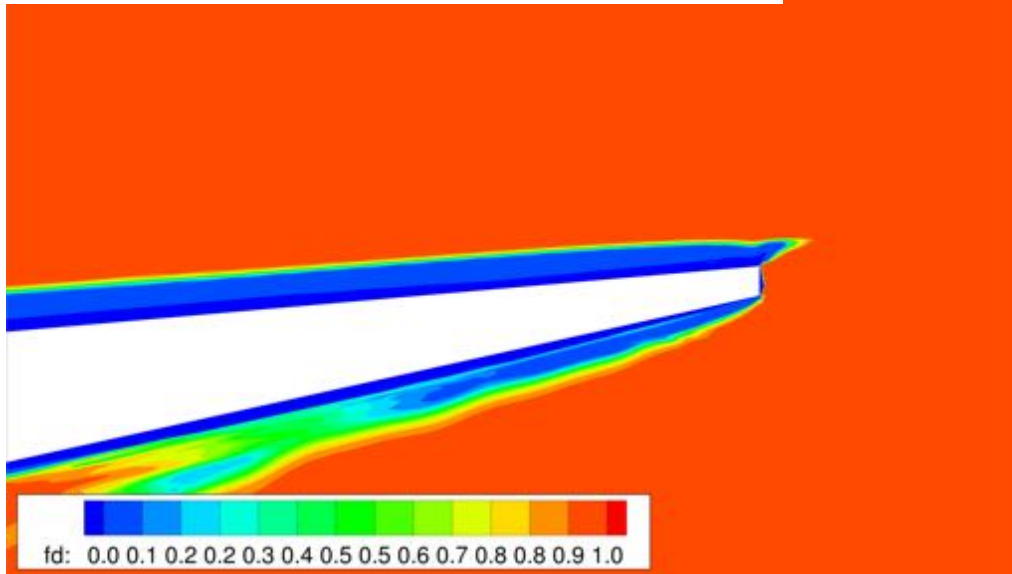
d_0 : transition distance (user)

ϵ_d : blending (user)

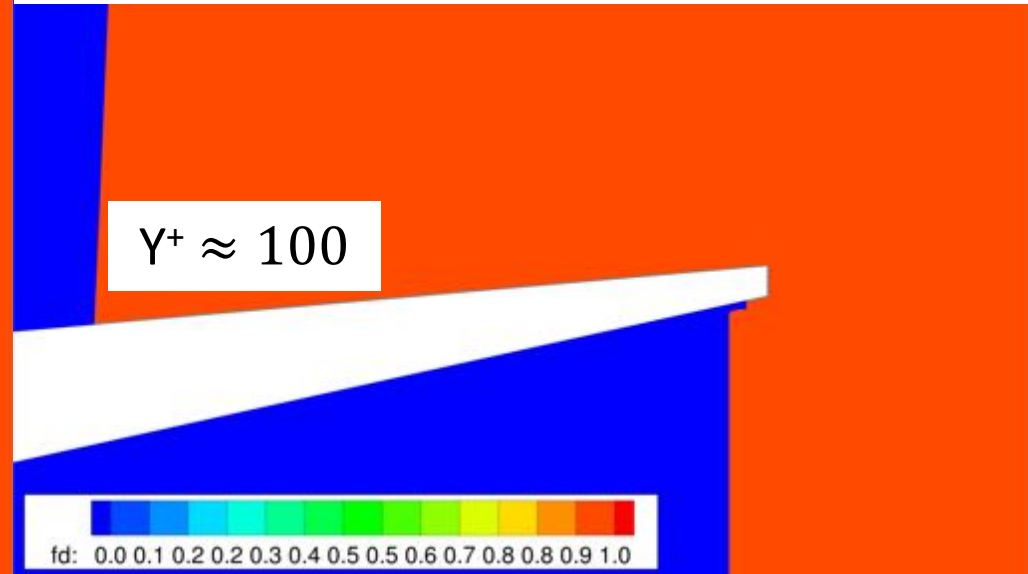
Computational Results



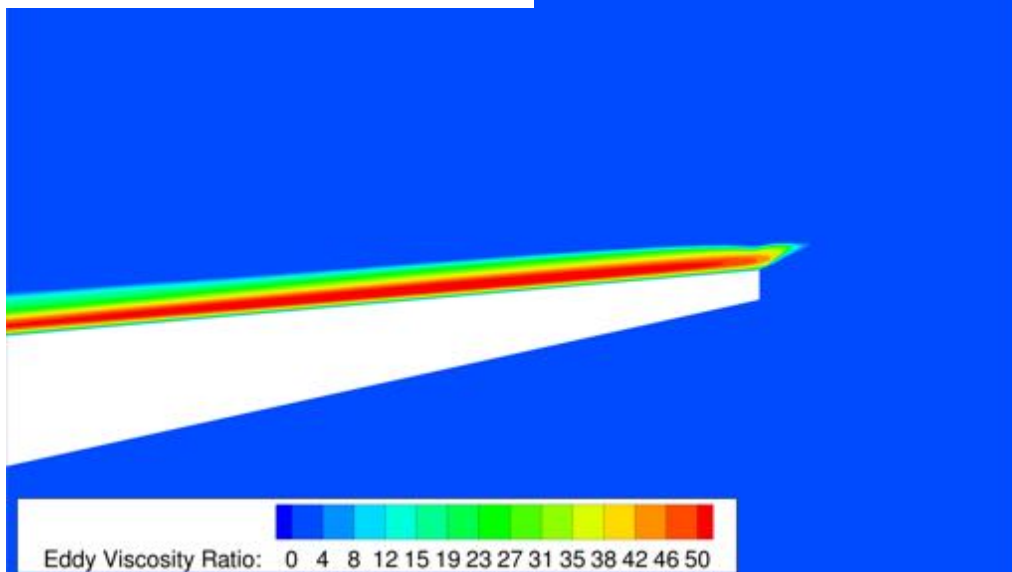
Indicator Function: DDES-256M



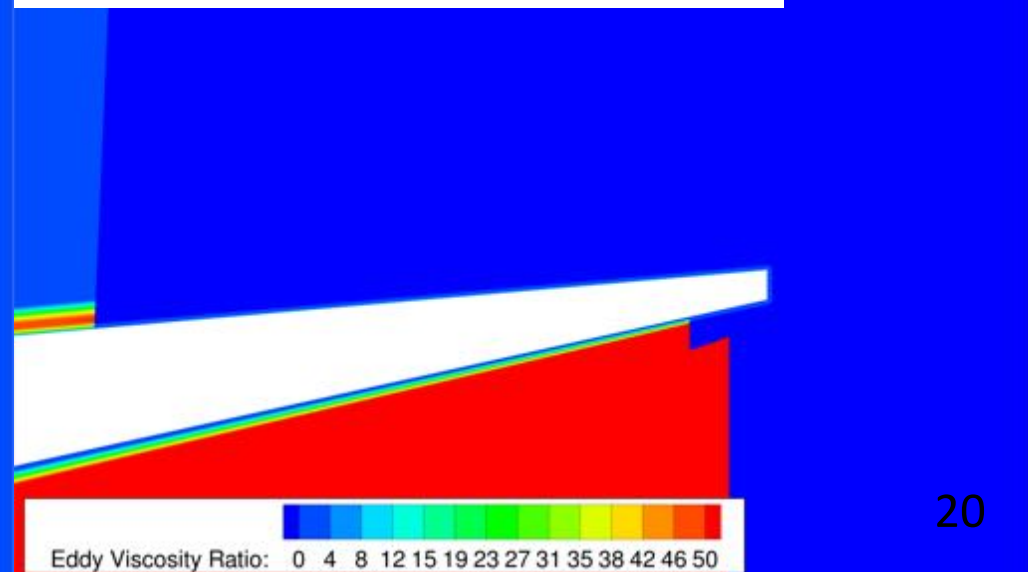
Indicator Function: RANS-NLES-SEM-106M



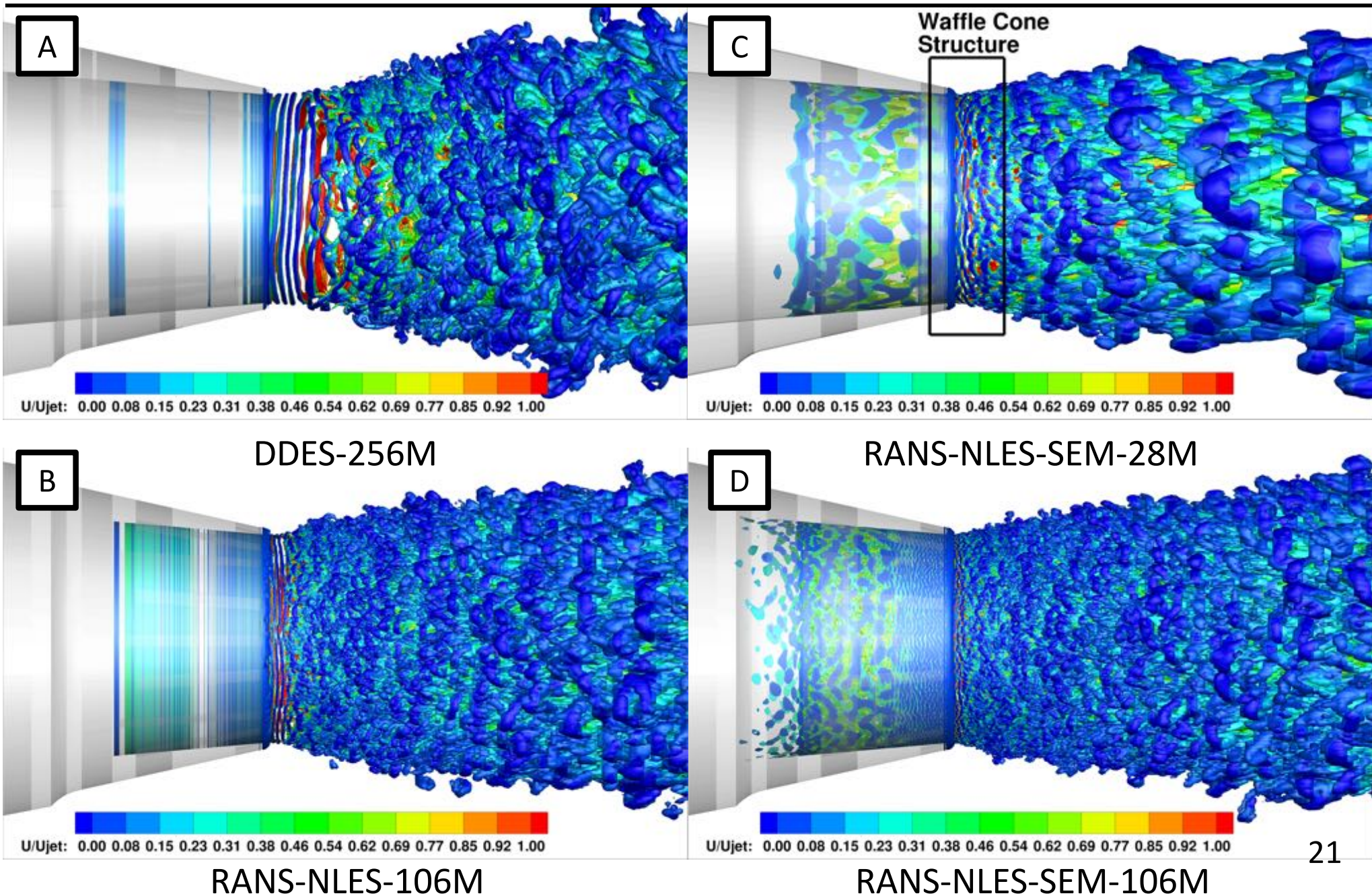
μ_T/μ_∞ : DDES-256M



μ_T/μ_∞ : RANS-NLES-SEM-106M



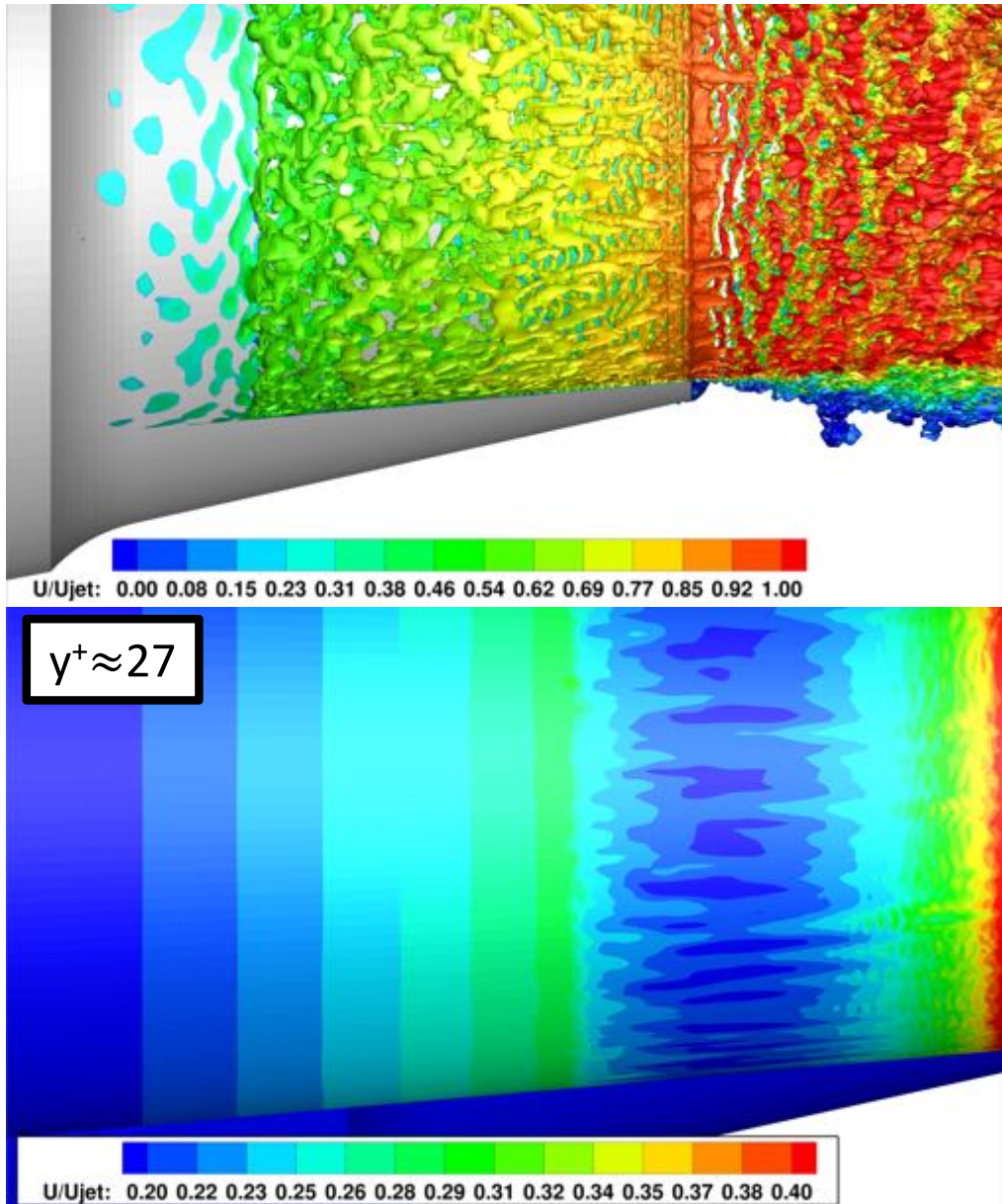
Computational Results



Computational Results



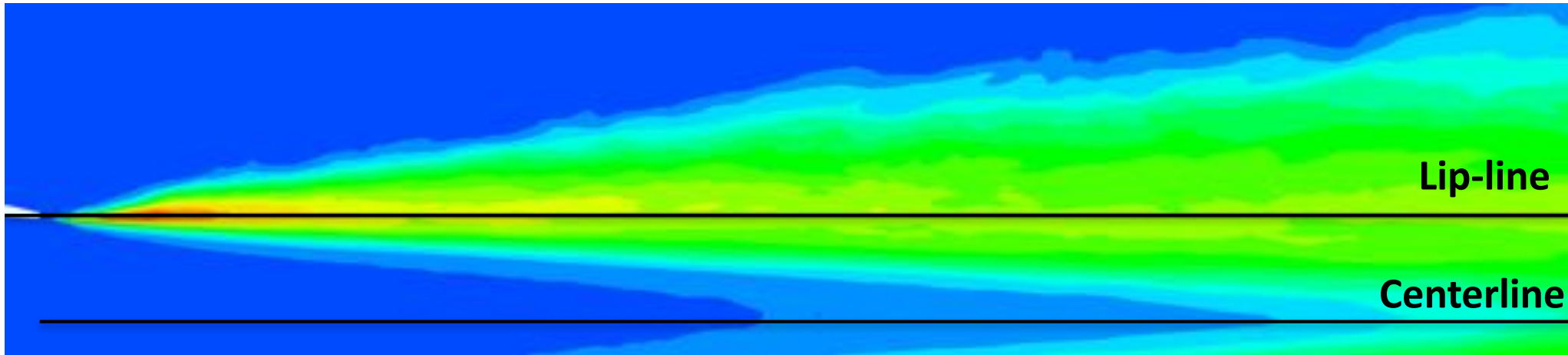
RANS-NLES-SEM Refined Mesh



- Quasi-2D waffle cone structures at nozzle exit
- Size of turbulent structures appears to be too large inside nozzle
- Structures deep in the boundary layer show very little azimuthal variation
- Features are elongated and too highly correlated in both the streamwise and azimuthal direction
- *Do we have realistic, fully developed BL turbulence at exit?*

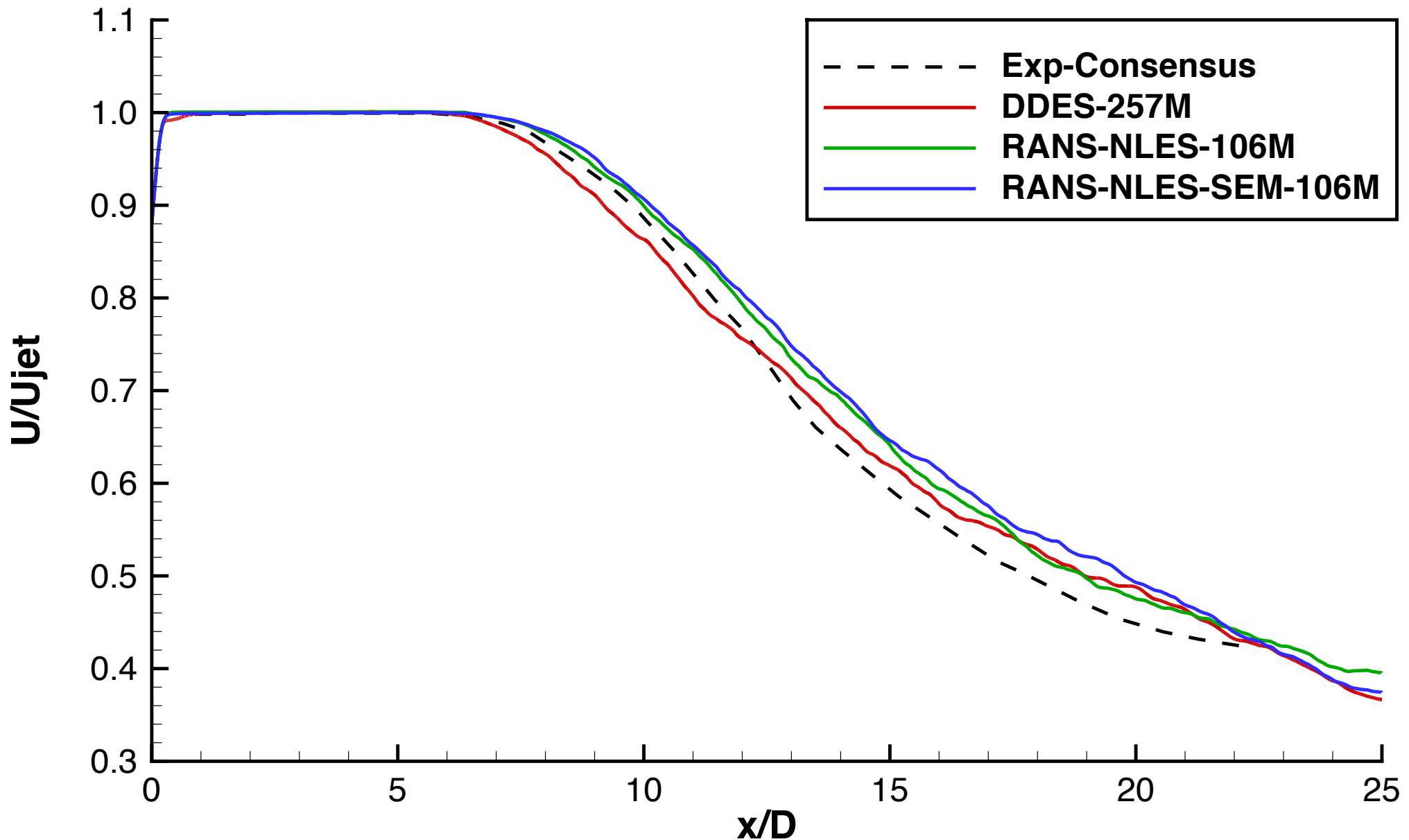
Computational Results – Near-Field

Near-Field Comparison



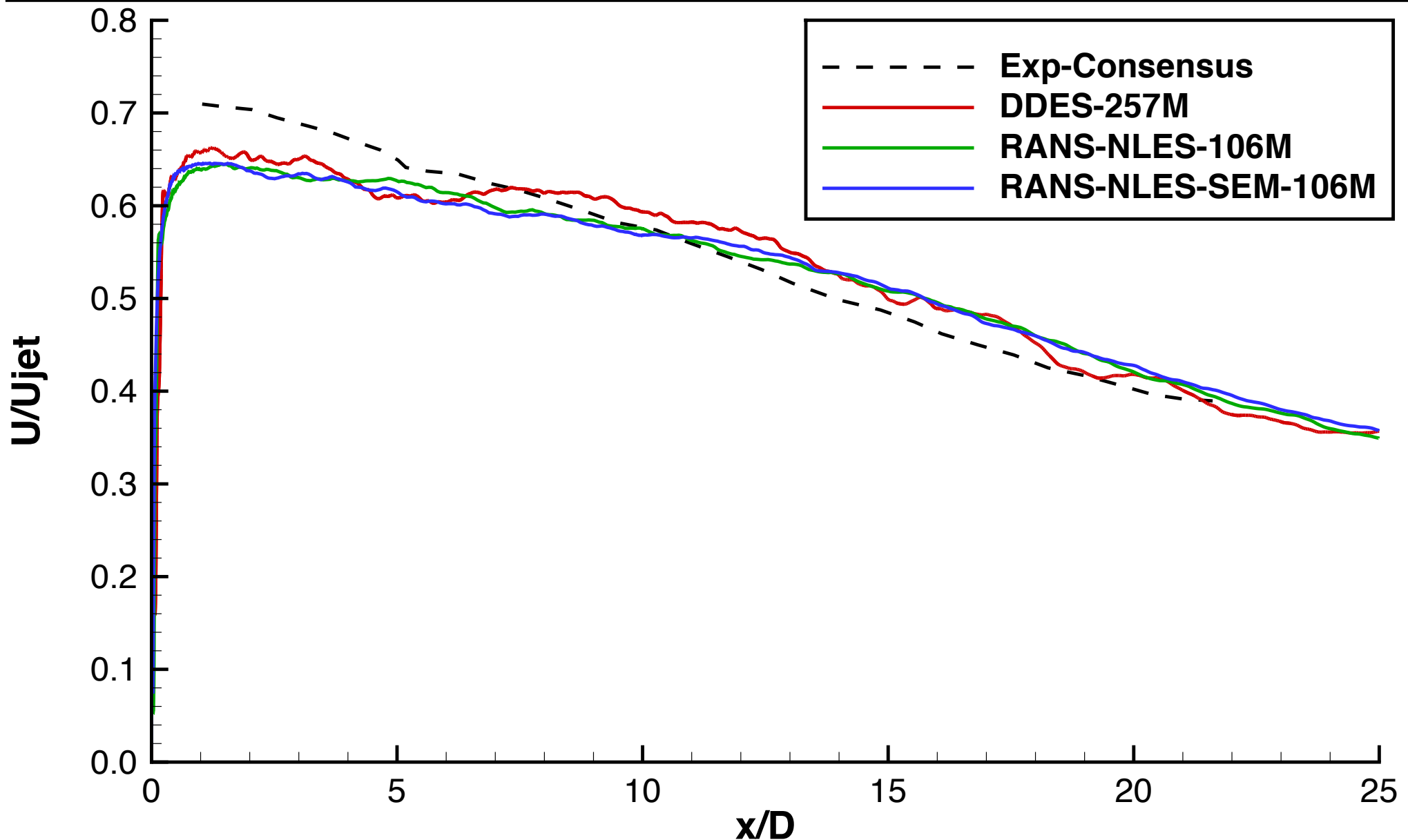
- Near field turbulent statistics computed from DDES, RANS-NLES and RANS-NLES-SEM models for comparison with PIV data from the SHJAR
- Comparison of measurements to data at lip-line ($z/R=1$) and Centerline ($z/R=0$)

Computational Results – Near-Field



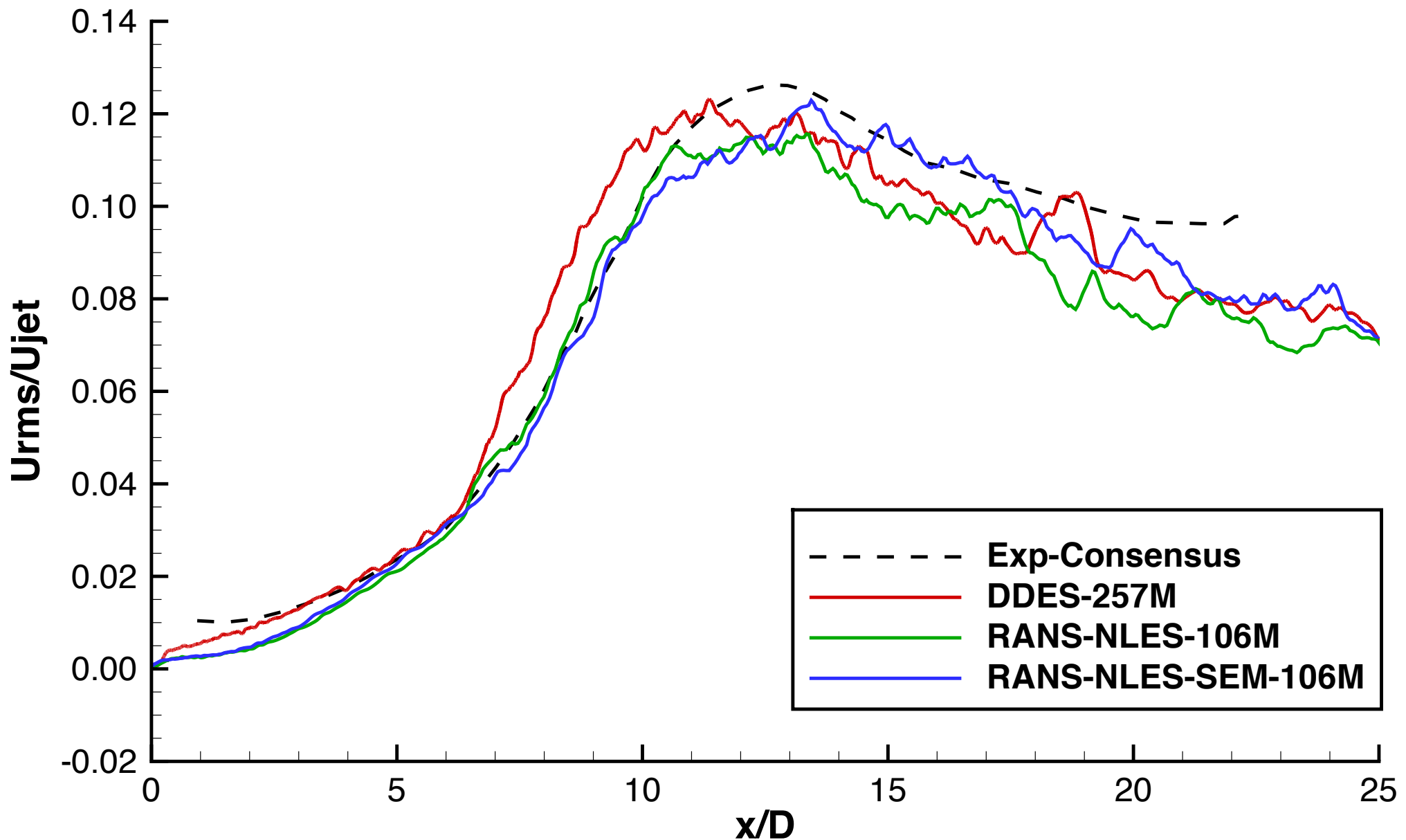
Near-Field Comparison: Time-Averaged Centerline

Computational Results – Near-Field



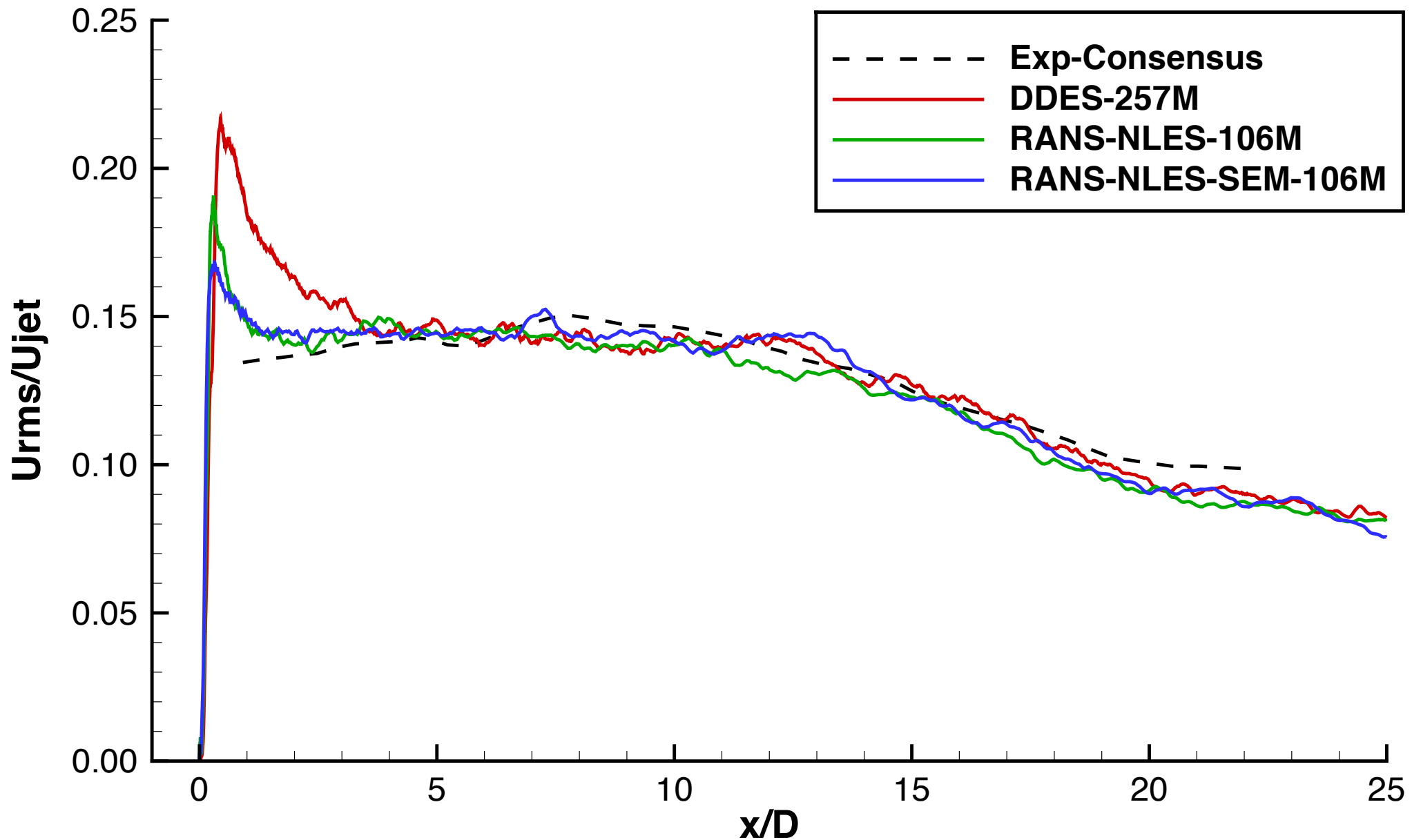
Near-Field Comparison: Time-Averaged Lip-line

Computational Results – Near-Field



Near-Field Comparison: RMS Centerline

Computational Results – Near-Field



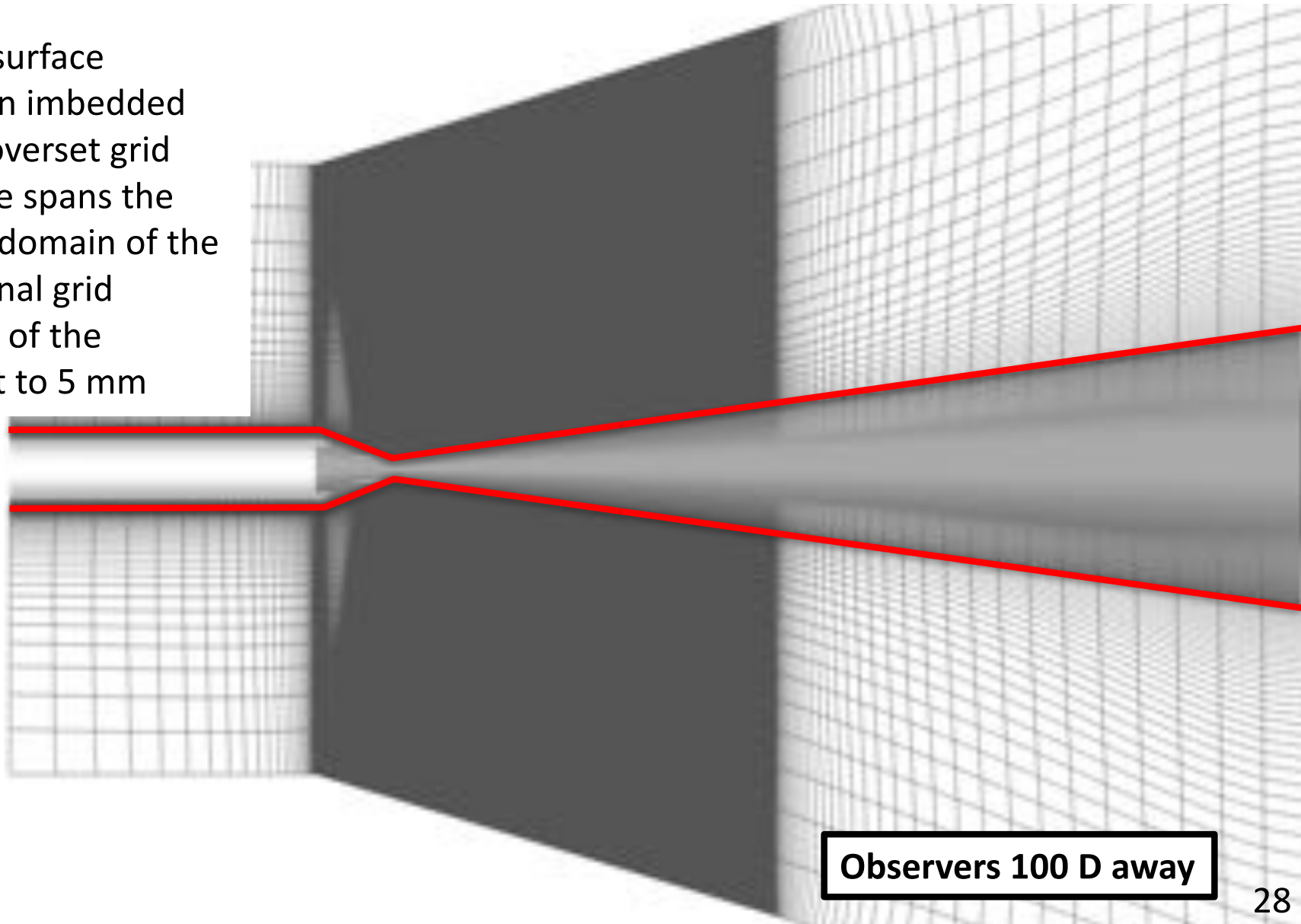
Near-Field Comparison: RMS Lip-line

Computational Results – Far-Field



FWH Permeable Surface

- Generated surface triangulation imbedded within the overset grid
- FWH surface spans the entire axial domain of the computational grid
- Edge length of the triangles set to 5 mm

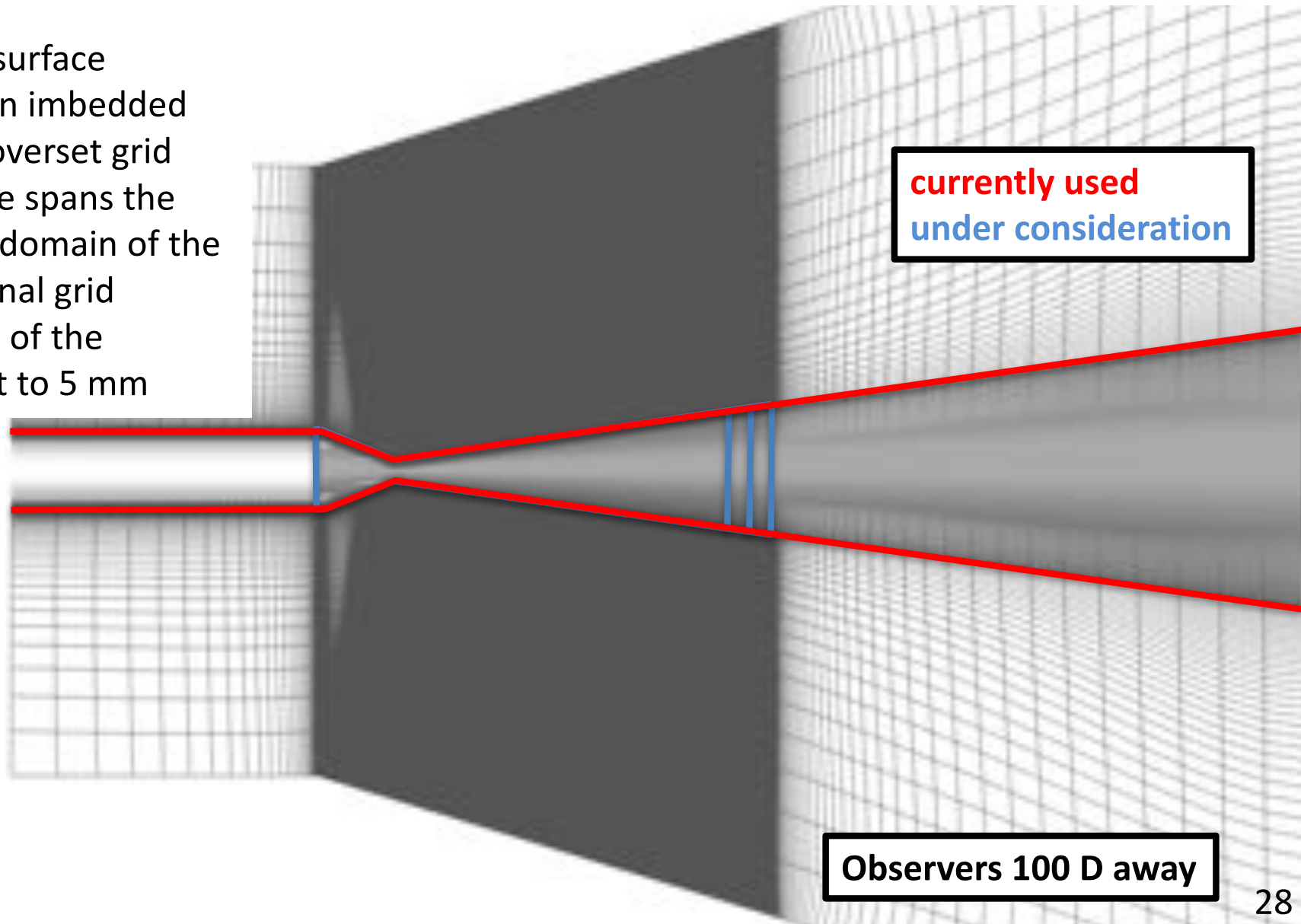


Computational Results – Far-Field



FWH Permeable Surface

- Generated surface triangulation imbedded within the overset grid
- FWH surface spans the entire axial domain of the computational grid
- Edge length of the triangles set to 5 mm

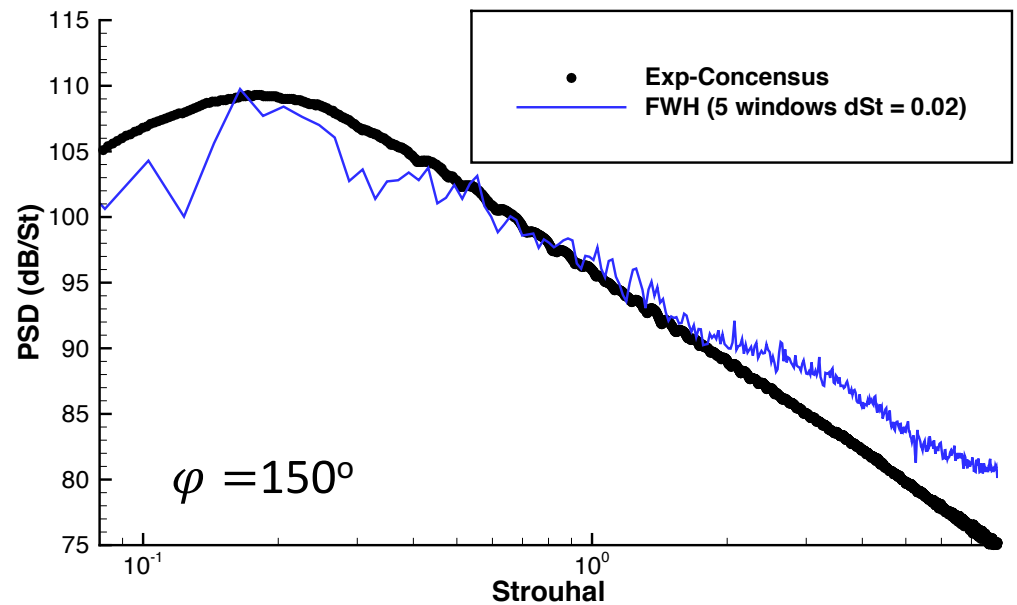
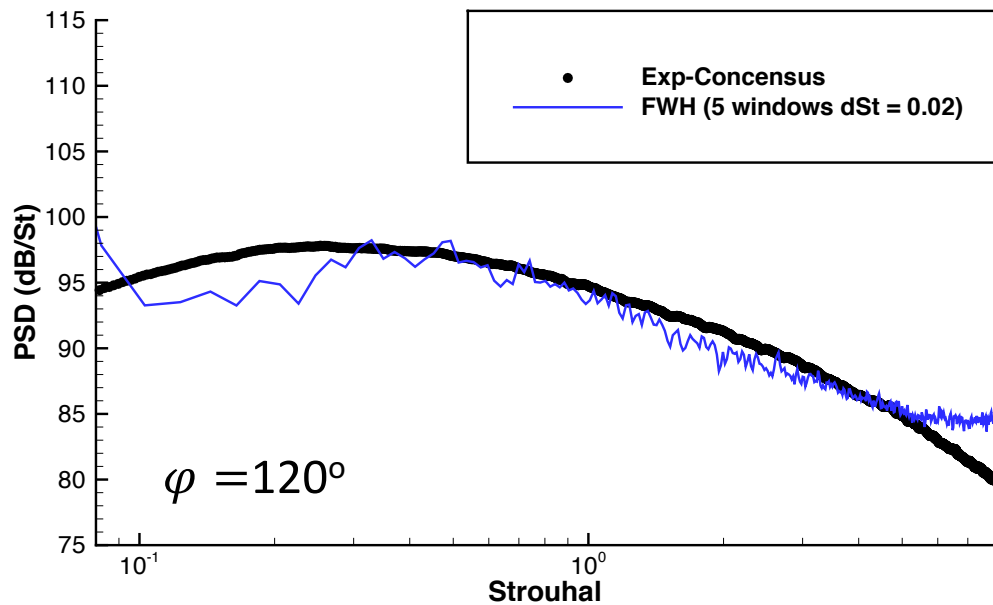
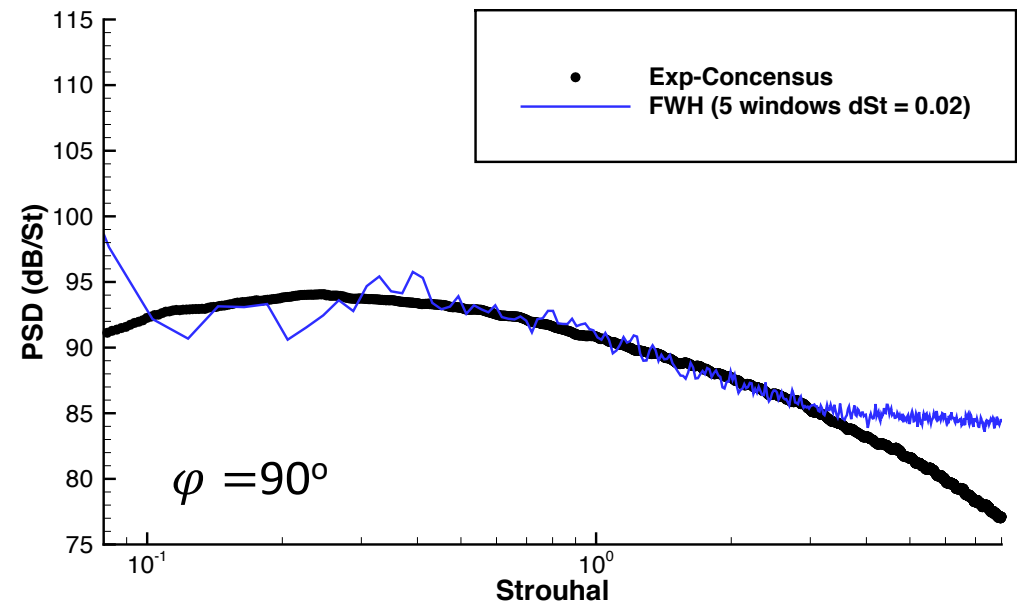
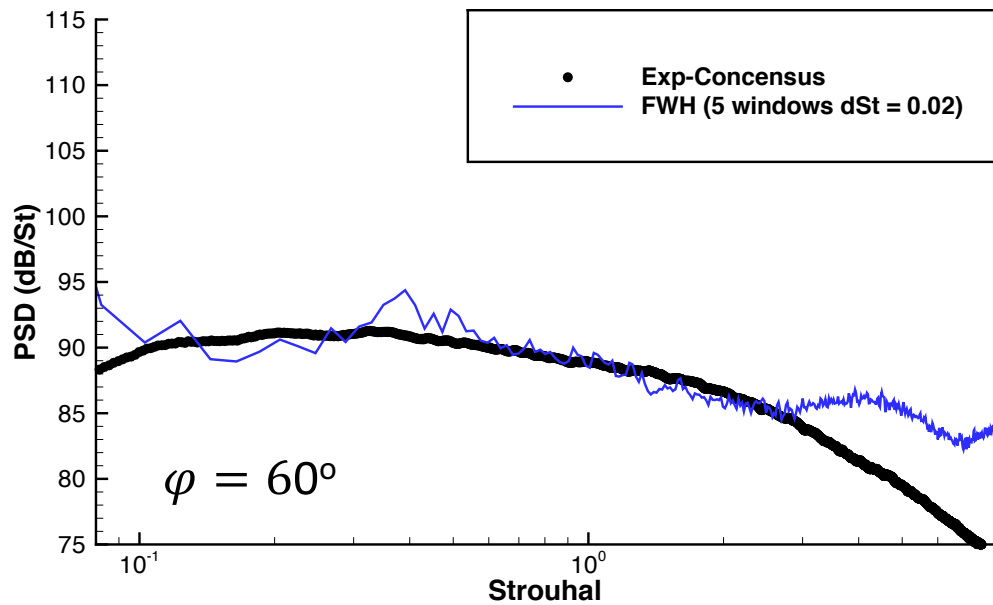


Computational Results – Far-Field



- Volume solution is interpolated to the FWH surface at a sampling rate of $\Delta t = 0.00001 \text{ s}$ (100 kHz)
- Total time sample is split into 5 windows (or segments) with 50% overlap at an $St_{\text{bin}} = 0.02$
- Integrands of the FWH permeable surface formulation are computed over each window independently
 - Q_n, F_1, F_2, F_3
 - Hanning Window is applied in the time-domain
 - FFT is applied and stored for computing far-field observer noise levels
- FWH surface integrals are computed for each observer over each window independently
 - 360 observers, uniformly distributed along the azimuth, are generated for each jet axis angle ($60^\circ, 90^\circ, 120^\circ, 150^\circ$)
 - The PSD is ensemble averaged over the 360 observers and the PSD is multiplied by $\sqrt{8/3}$ to recover the RMS levels lost from Hanning Window
- Finally, the PSD spectrum is averaged over the 5 windows for the final comparison to the experimental consensus.

Computational Results – Far-Field

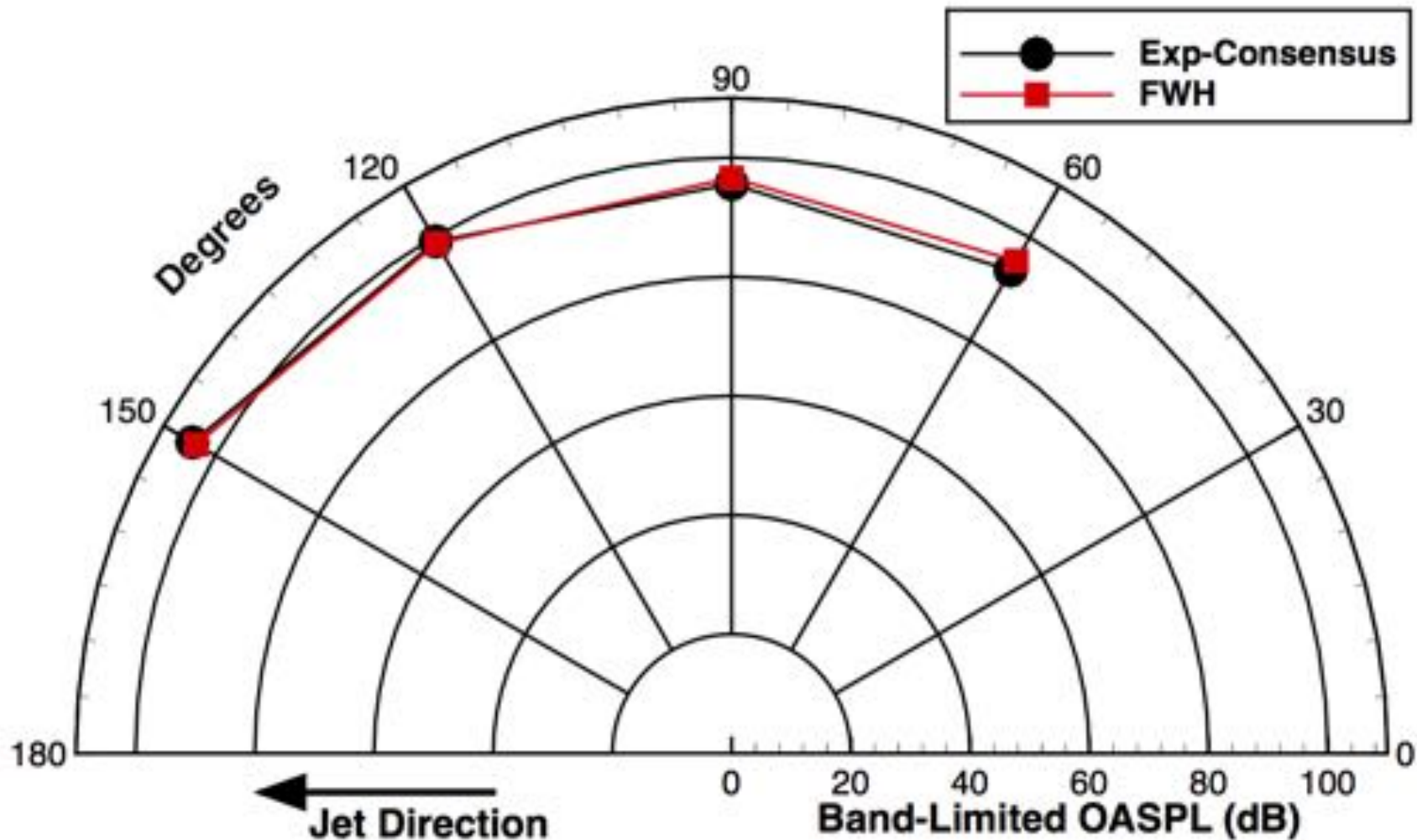


Far-Field Comparison: PSD Spectrum at 100D from exit

Computational Results – Far-Field



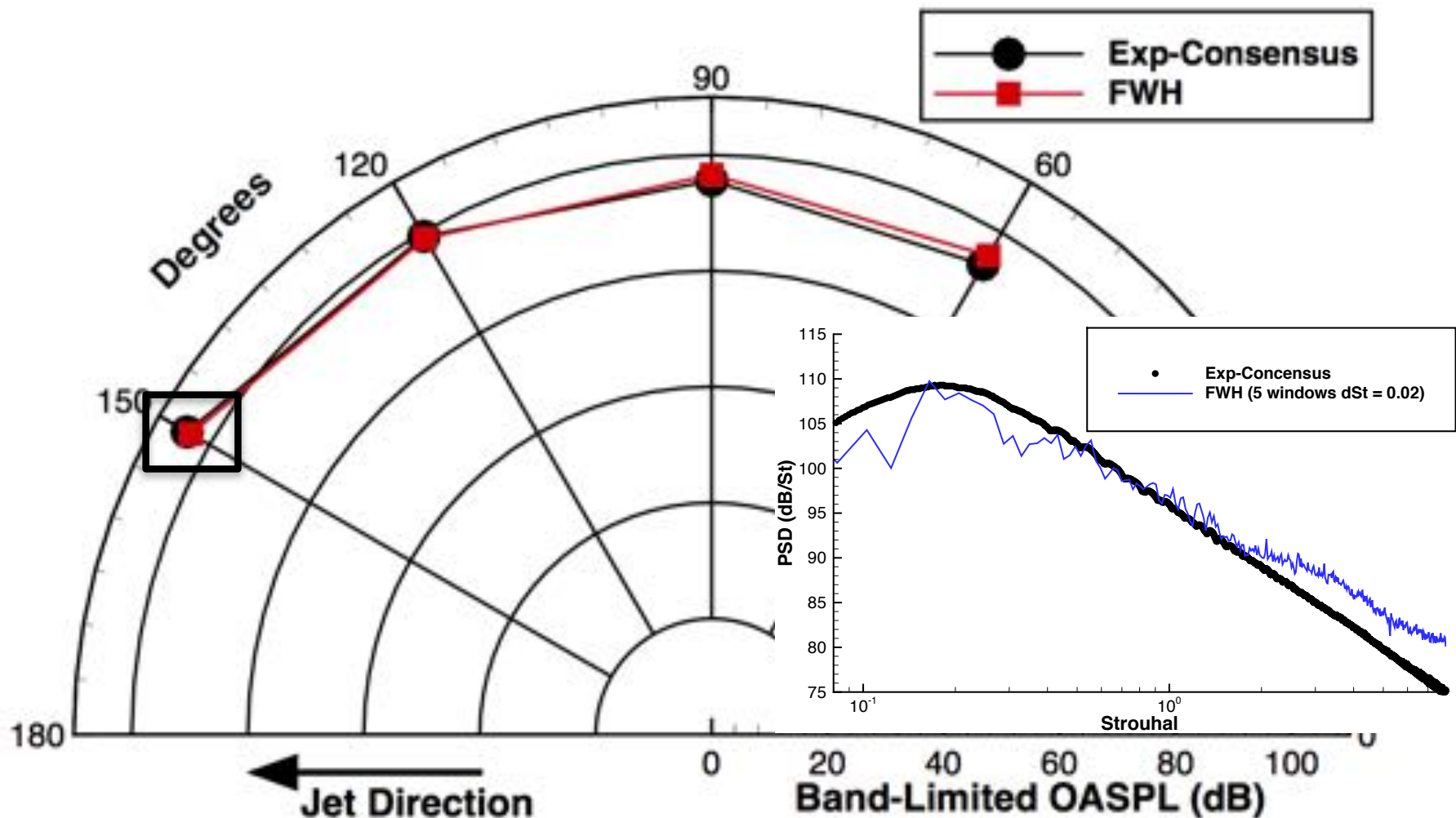
Far-Field Comparison: Band-Limited OASPL ($0.08 \leq St \leq 8.0$)



Computational Results – Far-Field



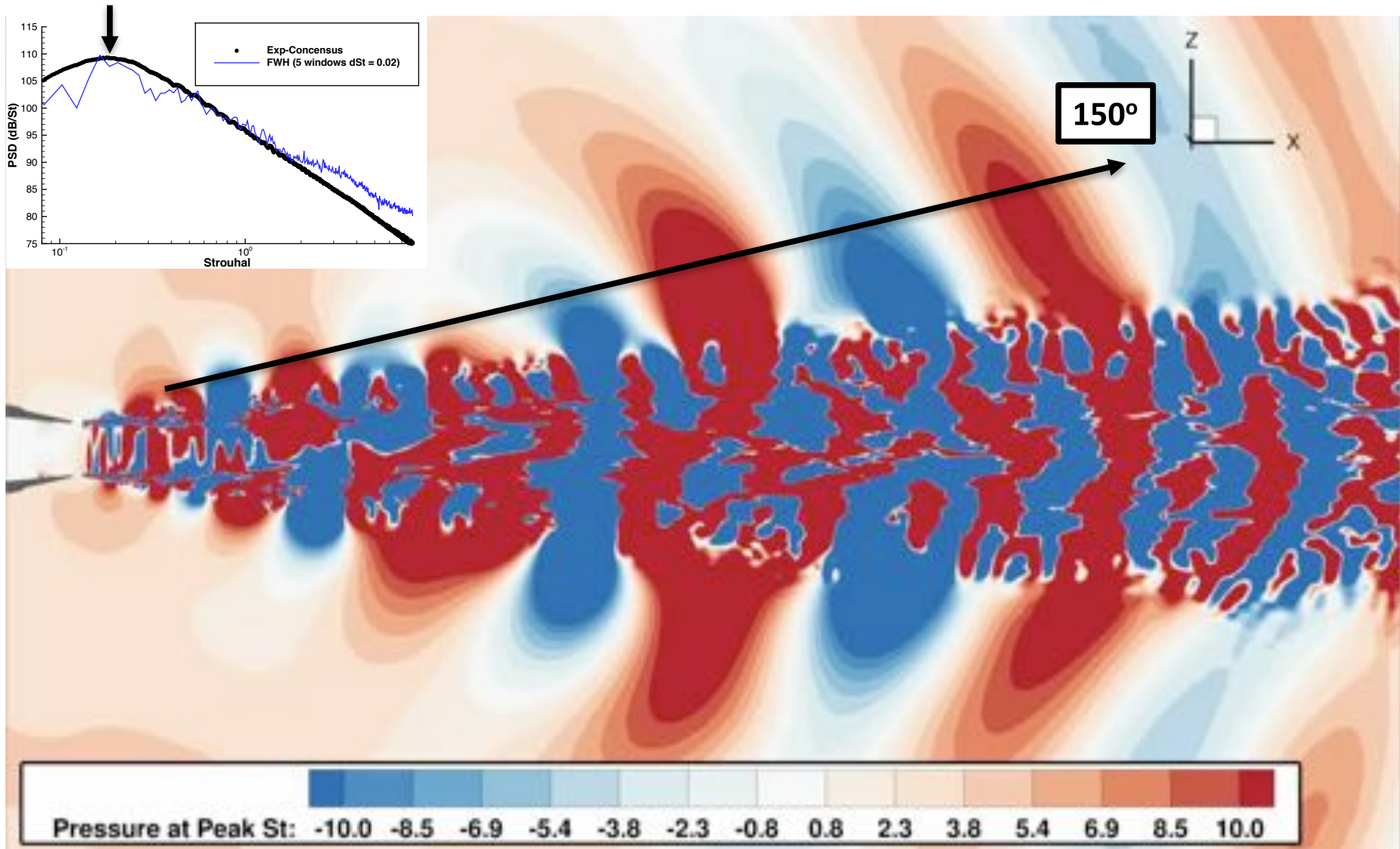
Far-Field Comparison: Band-Limited OASPL ($0.08 \leq St \leq 8.0$)



Computational Results – Far-Field



Time-Domain Pressure Associated with Peak Frequency (1100Hz) in 150°



Outline



- Introduction
- Experimental Setup
- Computational Methodology
- Structured Overset Grid System
- Computed Results
 - Near-Field Comparison
 - Far-Field Comparison
- **Summary**
- **Future Work**

Summary



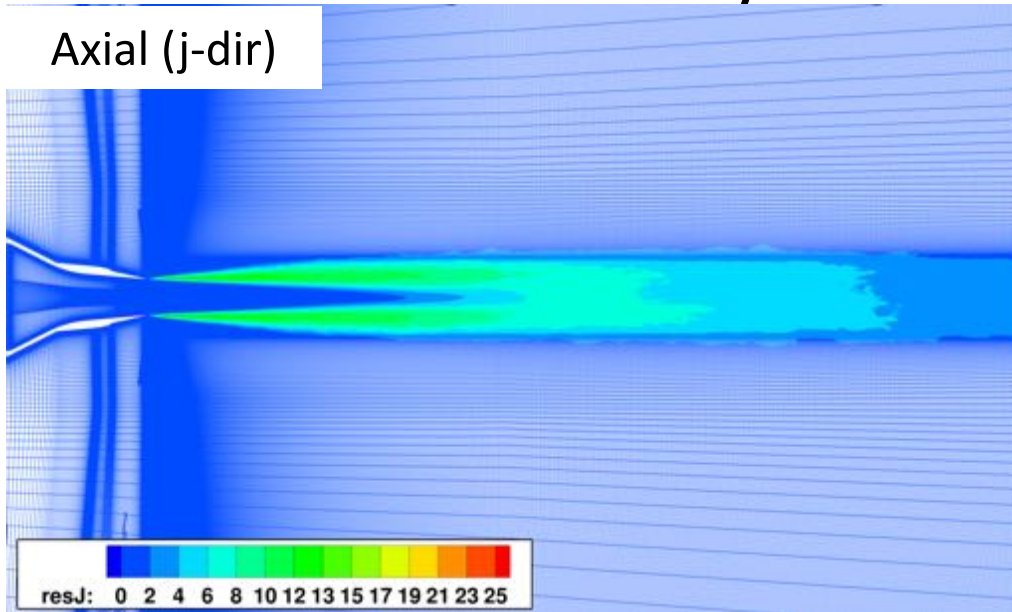
- The hybrid RANS/LES approach, within the LAVA framework, using structured curvilinear overlapping grids has been applied to the prediction of jet noise and compared to existing near-field PIV and far-field microphone data.
- Demonstrated improvements:
 - Hybrid RANS-NLES reduces the delay in transition to 3D turbulent structures and improved lip-line RMS prediction
 - SEM eliminates delay even further
- Completed far-field acoustic propagation
 - Mach wave radiation noise in the jet direction is well-captured
 - Sideline noise caused by turbulent fluctuations is over-predicted, likely do to elevated lip-line RMS at nozzle exit
- BL needs to be resolved better inside of nozzle for further improvements

Future Work

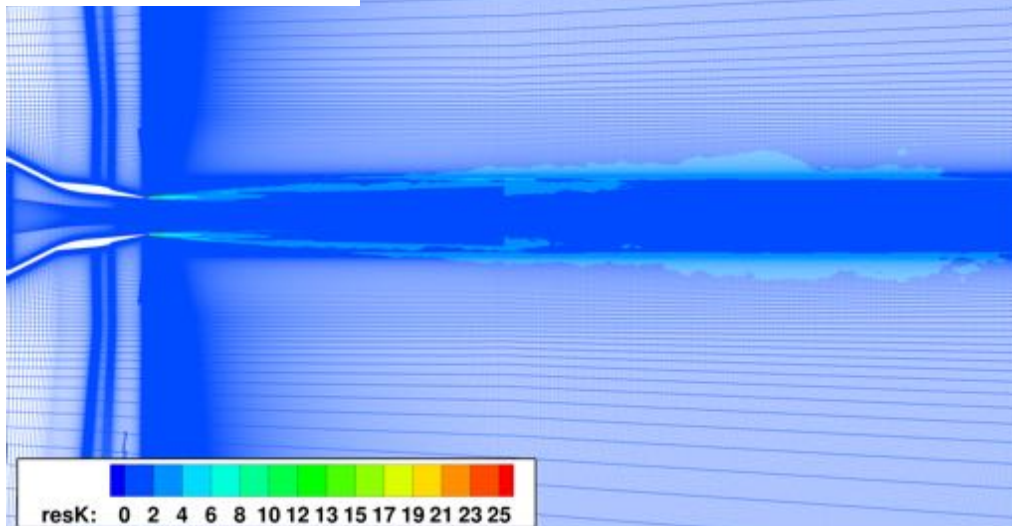


a Posteriori Error Analysis

Axial (j-dir)



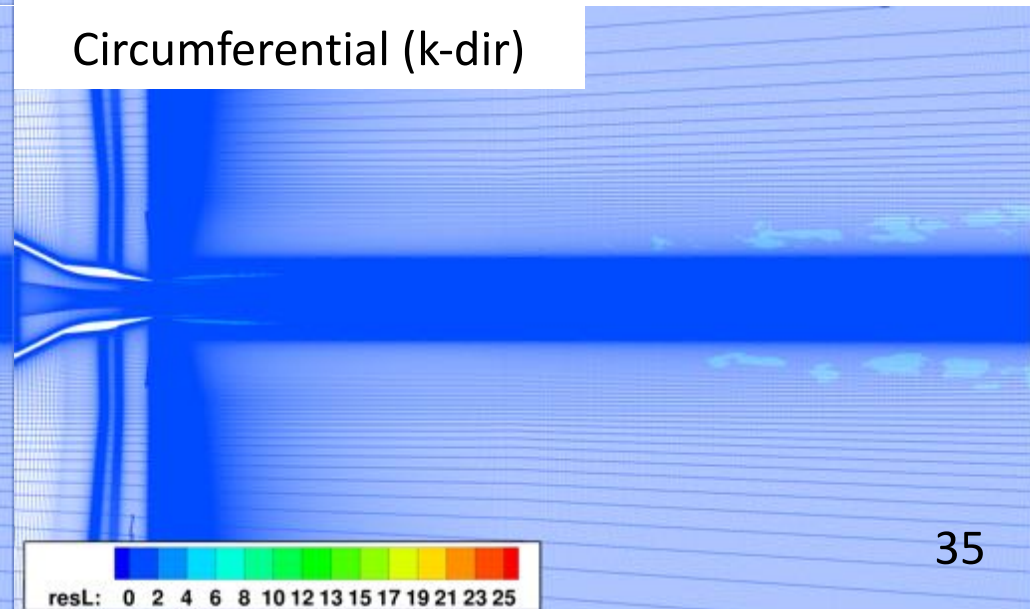
Radial (l-dir)



AIAA-2017-0978 Anisotropic grid-adaptation
in LES of wall-bounded and free shear flows,
Toosi and Larsson

- Analyze the difference in turbulent kinetic energy using the resolved velocity field with filtered version of resolved velocity field.
- Independent filtering in each direction leads to anisotropic measure for refinement

Circumferential (k-dir)

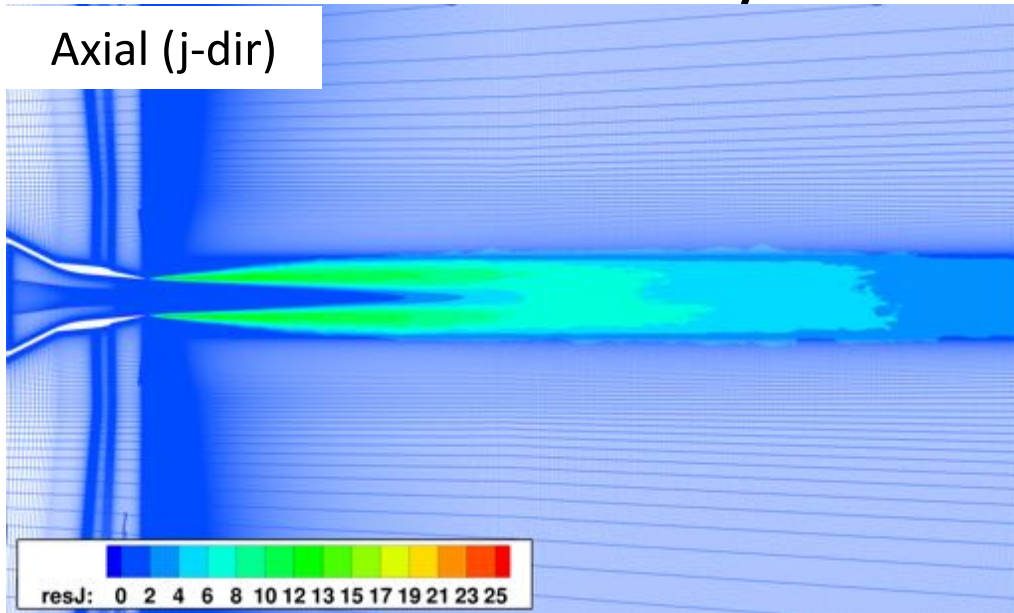


Future Work

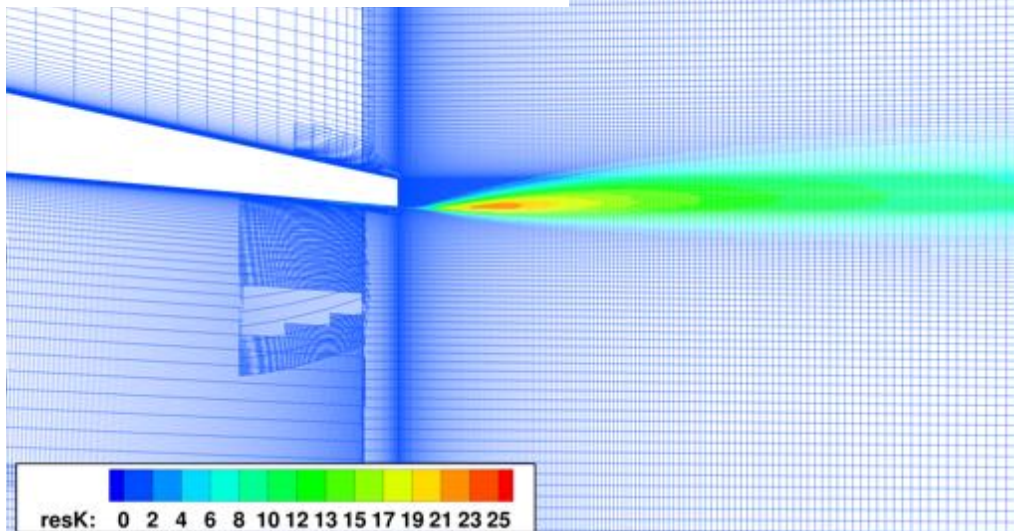


a Posteriori Error Analysis

Axial (j-dir)



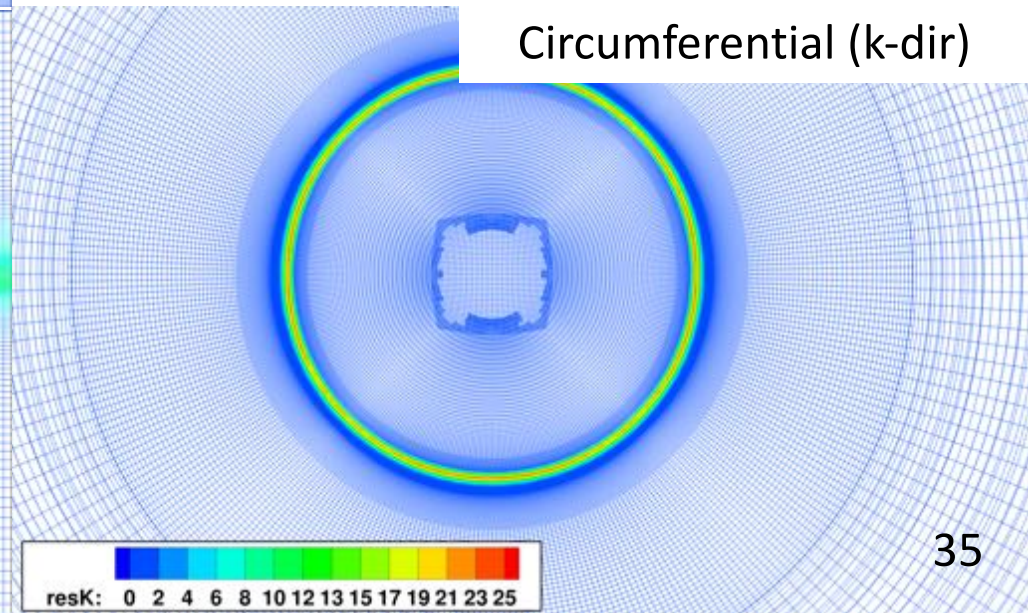
Circumferential (k-dir)



AIAA-2017-0978 Anisotropic grid-adaptation
in LES of wall-bounded and free shear flows,
Toosi and Larsson

- Resolution in streamwise direction is lacking the most.
- The error estimate has largest magnitude in circumferential direction.
- Radial direction pretty good.
- Improved mesh (191 M) for further investigation of SP7 and all SP3 runs

Circumferential (k-dir)



Future Work

LES with explicit subgrid-scale (SGS) model and SEM

We need wall-modeled LES in order to resolve the boundary layer inside the nozzle!

- No RANS downstream of SEM location
- Waffle cone structures inside nozzle reduced
- Artificial turbulence from SEM decays towards nozzle exit due to lack of resolution
- Recommended resolution:
wall-resolved $\Delta s_{circ}^+ = 20$
(12.5k points)
wall-modeled $\Delta s_{circ} = 0.1\delta$
(2450 points)

QUESTION:

"How will SGS model affect our lipline RMS and farfield solutions"

U/Ujet: 0.0 0.1 0.2 0.2 0.3 0.4 0.5 0.5 0.6 0.7 0.8 0.8 0.9 1.0

Acknowledgements



- This work was also partially funded by the Commercial Supersonics Technology (CST) project and the Transformational Tools and Technology (T³) project under the Aeronautics Research Mission Directorate (ARMD).
- Computer time has been provided by the NASA Advanced Supercomputing (NAS) facility at NASA Ames Research Center.
- Patrick J. Morran from NASA Ames visualization team for rendering of numerical schlieren video.
- Team members of LAVA group for helpful discussions and advise: Joseph George Kocheemoolayil, Francois Cadieux, Michael Barad

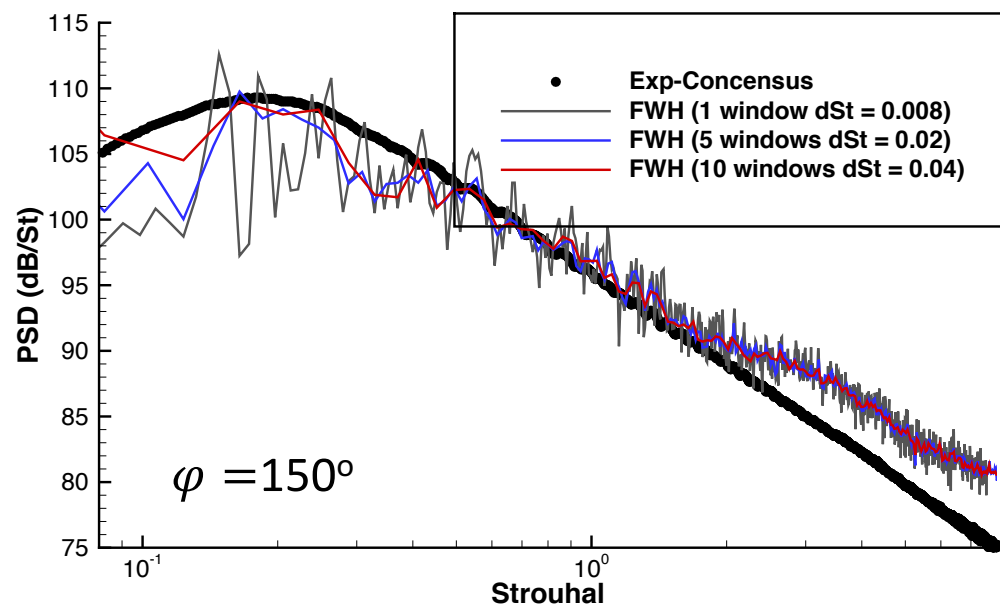
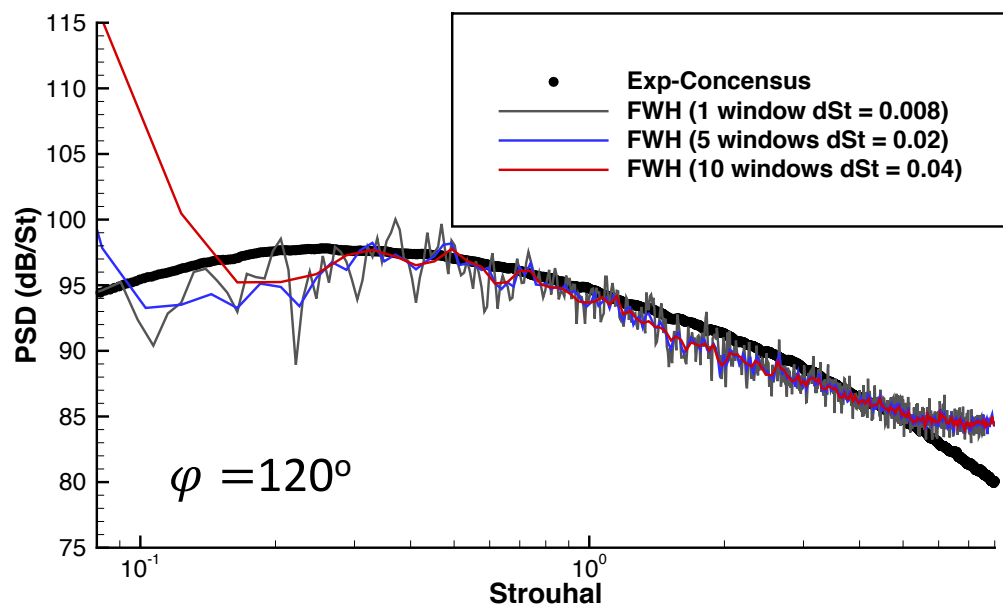
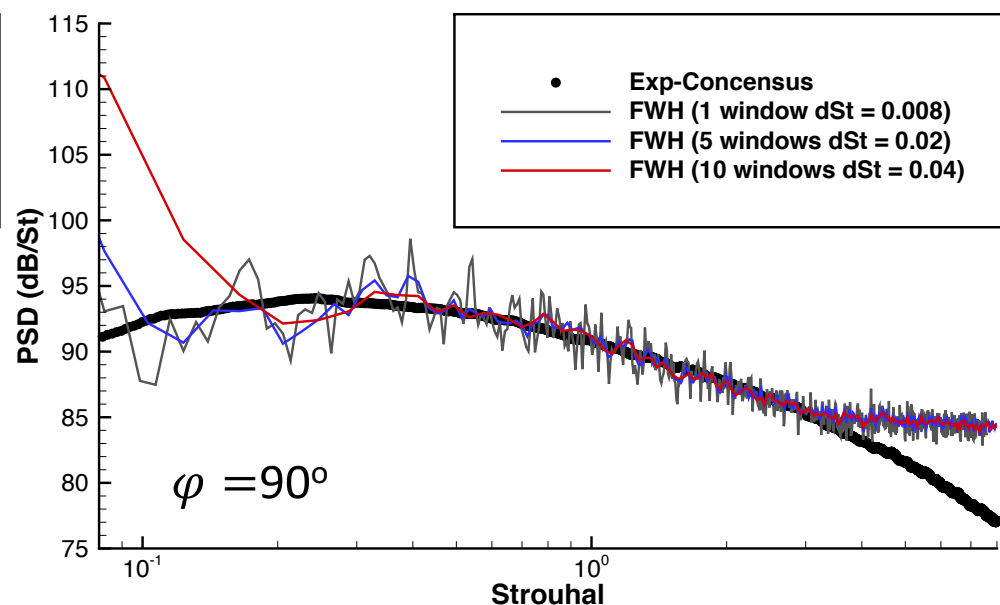
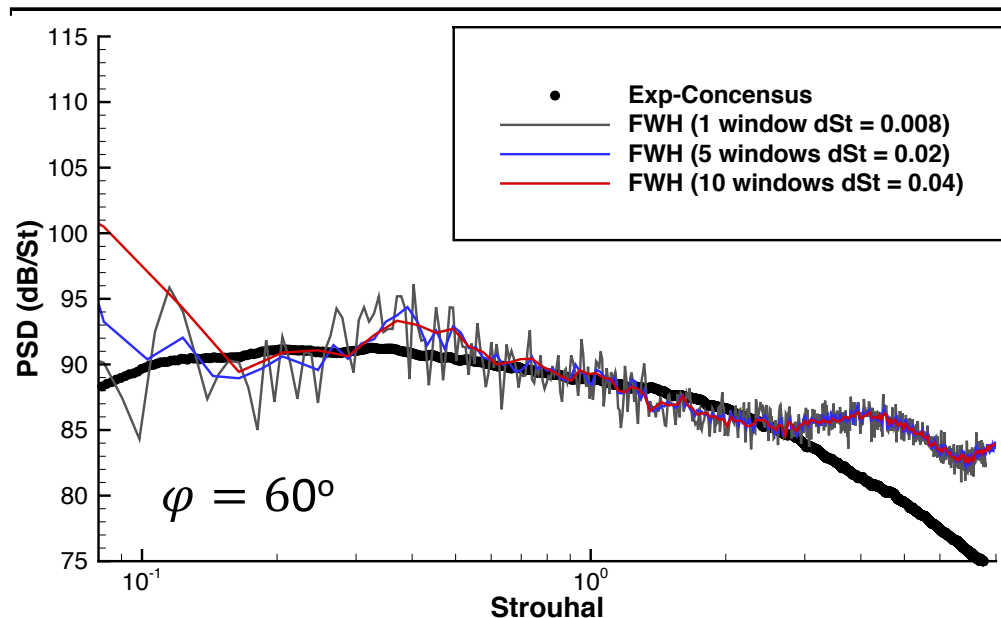
Questions?



BACKUP

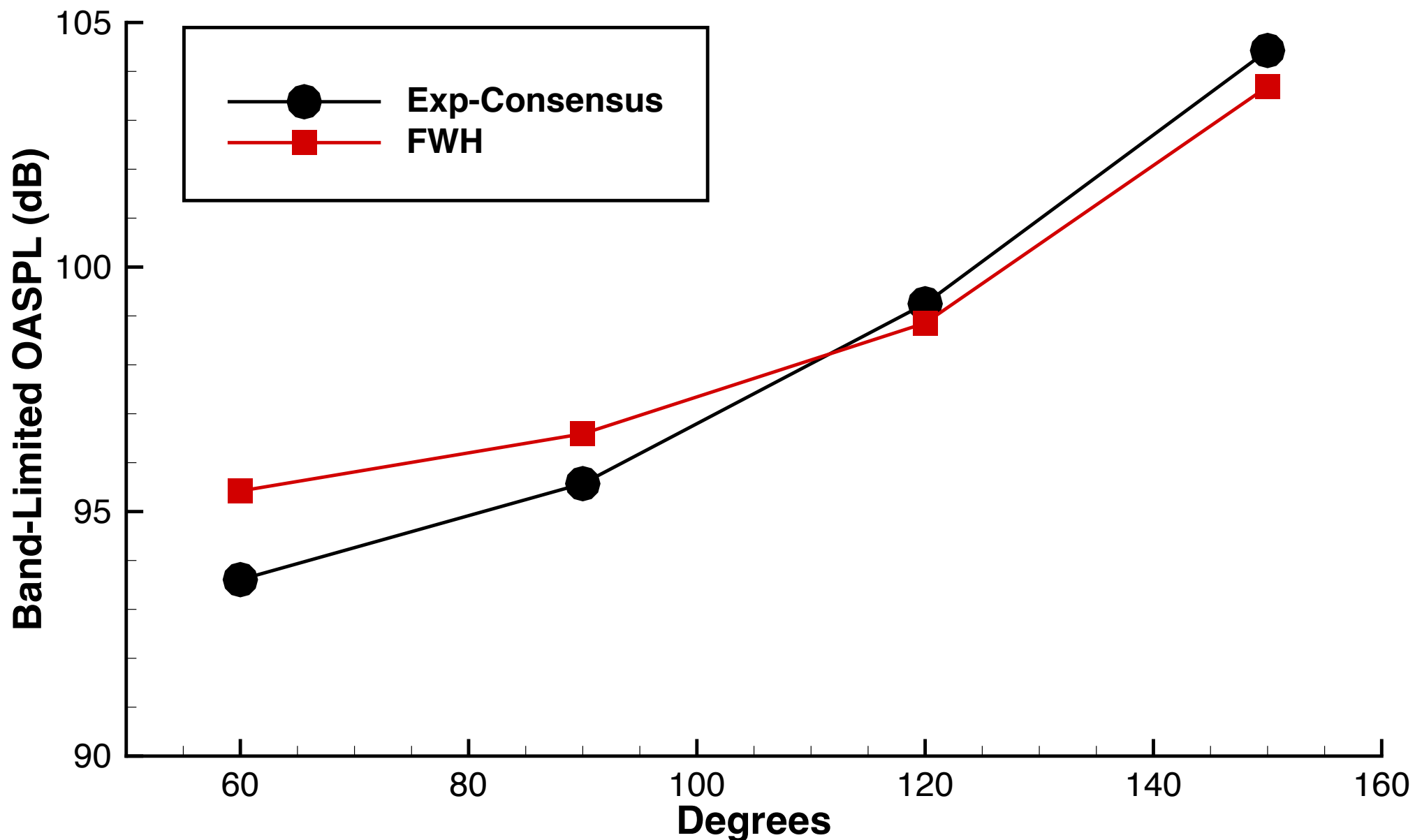


BACKUP



Far-Field Comparison: PSD Spectrum at 100D from exit

BACKUP



Far-Field Comparison: Band-Limited OASPL ($0.08 \leq St \leq 8.0$) ⁴⁸

BACKUP



SEM backup slide. See former presentation from last year when I added the SEM routines

Add slide for different turbulent inflow methods. Comparison name of Spalarts SGT Maybe friction velocity plot.

BACKUP



EXACT LOCATION OF MICROPHONE POSITIONS

BACKUP



End cap averaging for FWH surface. Add more info in correspondence with Joseph.